

REGENERATING VASCULARIZED CRANIOFACIAL BONE FROM  
3D-PRINTED SCAFFOLDS AND STROMAL-VASCULAR FRACTION CELLS:  
AN ANIMATION AND INTERACTIVE PRESENTATION  
FOR LAY AUDIENCE AND SCIENTISTS

by  
Kai-ou Tang

A thesis submitted to Johns Hopkins University in conformity  
with the requirements for the degree of Master of Arts

Baltimore, Maryland  
March, 2016

© 2016 Kai-ou Tang  
All Rights Reserved

## ABSTRACT

Present day surgical reconstruction of large craniofacial defects relies on bone grafts to restore the patient's facial structure and function. However, this procedure is limited in success due to the complex orbital, maxillary, zygomatic, and mandibular structure of the craniofacial area. The most effective post-surgical patient social reintegration correlates not only to the anatomical and physiological outcomes of the surgery, but also its cosmetic results.

To this end, biomaterials and medical research proposes a 3D printed scaffold customized to fit the patient. However, there are currently no existing visualizations to explain the complex science of this procedure, hindering progress both in how the research is communicated, as well as opportunities for funding and research.

To fulfill the lack of biovisualization material pertaining to 3D printed scaffolds, a presentation animation was created using a combination of 2D and 3D assets, as well as 3D models extracted from CT scans. The resulting MPG4 animation files were created using a combination of Osirix reconstruction software and edited using Zbrush digital sculpting software. Assets were then imported into Cinema 4D modeling/animation software and AfterEffects compositing and animation software. In addition, a browser-based interactive presentation was made with the purpose of elucidating the cellular process of angiogenesis. An interactive presentation of angiogenesis was also made with 3D models, and implemented through HTML and Javascript. The presentation was created to be viewed using standard browser applications for ease of access, without the need for plugins or file distribution.

The creation of these visualizations addresses the advantages of 3D printed scaffolds compared to current surgical bone graft methods, as well as the visualization and rate at which the bone would become vascularized, in order to communicate the current state of craniofacial reconstruction research. The animation and interactive presentation produced as a result of this project not only allows both the layman and

scientist to understand and learn about 3D printed bony scaffolds, but also brings attention to the rapidly progressing field of medical biomaterials. This research further highlights the potential and need for biovisualizations to burgeon alongside this exciting frontier of medical research.

Author: **Kai-ou Tang**, MA Candidate

Advisor: **Juan R. Garcia**, MA, CCA, Associate Professor

The Department of Art as Applied to Medicine

Johns Hopkins School of Medicine

Preceptor: **Warren Grayson**, PhD

Department of Biomedical Engineering

Johns Hopkins School of Medicine

## ACKNOWLEDGMENTS

The following individuals contributed significantly to the success and goals of this thesis. I would sincerely like to thank:

**Warren Grayson, PhD**, Assistant Professor, Department of Biomedical Engineering, Johns Hopkins Biomedical Engineering, and my preceptor, for his work in the field of biomaterials and bone grafting. Thank you for granting access to your laboratory, knowledge on the subject, and for helping shape my thesis.

**Juan R. Garcia, MA, CCA**, Associate Professor, Department of Arts as Applied to Medicine, Johns Hopkins University School of Medicine, and my thesis advisor. For your critical eye in biocommunication and dedication as an instructor. Thank you for your direction and invaluable input in the making of this thesis.

**Ethan Nyberg**, and **Ben Hung**, Department of Biomedical Engineering, Johns Hopkins Biomedical Engineering, for sharing their laboratory and experiments with me, and helping me attain the information used to demonstrate the concept.

**Sarah Poynton, PhD**, Associate Professor, Molecular and Comparative Pathobiology and joint appointment at Department of Arts as Applied to Medicine, Johns Hopkins University School of Medicine. For her encouragement and positivity, as well as her key points on scientific writing and emphasis on clarity.

**The Vesalius Trust**. To the committee for furthering the field of biocommunication and recognizing medical illustration students. Thank you for the honor of being awarded the Vesalius Trust Research Grant.

**Gary Lees, MS, CMI**, Chairman, Associate Professor, and **Corinne Sandone, MA, CMI**, Director, Associate Professor, Department of Arts as Applied to Medicine, Johns Hopkins University School of Medicine, for their endless guidance and support throughout the course of the program, for which I cannot express enough gratitude.

**The Class of 2016**, Department of Arts as Applied to Medicine, Johns Hopkins University School of Medicine, thank you for the memories and late nights together.

# TABLE OF CONTENTS

<b>Abstract</b>	<i>ii</i>
<b>Acknowledgements</b>	<i>iv</i>
<b>Table of Contents</b>	<i>v</i>
<b>Index of Tables and Figures</b>	<i>vii</i>
<b>Introduction</b>	
Background	1
Problem Statement	2
Objectives	2
Audience	3
<b>Materials and Methods</b>	
Overview	4
Scaffold Contents: Setting and Scale	4
Narration	5
Storyboards	6
Asset Creation (2D Visual Elements)	7
CT Scan Sequence	7
Asset Creation of 3D Models	8
Optimized Approaches to Biovisualization	13
3D Animation	17
Compositing and Final Rendering	17
Angiogenesis Interactive Presentation	17
<b>Results and Discussion</b>	
Goals	21
Part I: An Anatomically-Shaped Graft is Essential for Functional Craniofacial Bone Regeneration	21
Part II: The 3D-Printed Scaffold Before Implantation	26
Part III: The Regeneration Process from 3D-printed Scaffold to Organic Bone Tissue	27
Part IV: The Workflow from CT Scan to Operation	28
Part V: Angiogenesis Interactive Presentation	29
Angiogenesis Feedback	31
Access to assets resulting from this thesis	33
<b>Conclusion</b>	34

# TABLE OF CONTENTS

<b>Appendix</b>	
Appendix A. List of Software and Hardware	35
Appendix B. Results in Storyboard Format	36
Appendix C. Angiogenesis Interactive: HTML and Javascript code	39
Appendix D. Part I Animation Storyboards	41
Appendix E. Part II Animation Storyboards	43
Appendix F. Part III Animation Storyboards	45
Appendix G. Part IV Animation Storyboards	46
Appendix H. Part V Angiogenesis Interactive Presentation	48
Appendix I. Part V Angiogenesis Interactive Presentation Time Lapse	49
Appendix J. Part I-IV Narration Script	51
<b>References</b>	55
<b>Vita</b>	57

## INDEX OF TABLES AND FIGURES

<b>Page</b>	<b>Figure</b>
5	Figure 1. Porous scaffold model
6	Figure 2. Narration file
6	Figure 3. Storyboards for Part I
7	Figure 4A and 4B. Silhouette, skeleton, and PSD layers
7	Figure 5. OsiriX MANIX DICOM screen
8	Figure 6. Skull model in ZBrush
9	Figure 7. Injured skull model
9	Figure 8. Final skull and teeth models
10	Figure 9. 3D-printed scaffold model
10	Figure 10. Porous scaffold model with lighting
11	Figure 11. Fibrin model test
12	Figure 12. Oxygen microtanks
12	Figure 13. Oxygen microtank in space
13	Figure 14. Adipose-derived stem cell UV map
13	Figure 15. Adipose-derived stem cell models with texture
14	Figure 16A and 16B. Scaffold model with boole function
15	Figure 17A, 17B, and 17C. Angiogenesis animation stills
16	Figure 18. Angiogenesis final layout
16	Figure 19. Angiogenesis in Object Manager
18	Figure 20. Angiogenesis MP4 HTML
18	Figure 21. Label text HTML
19	Figure 22. Normoxia vs. Hypoxia HTML
19	Figure 23. Angiogenesis Javascript
21	Figure 24. Bone grafts animation still
22	Figure 25. Autograft animation still
22	Figure 26. Autograft constraints animation still
23	Figure 27. 3D printed scaffold animation still

24	Figure 28. CT scan animation still
24	Figure 29. 3D model animation still
25	Figure 30. 3D printing animation still
25	Figure 31. Cell seeding animation still
26	Figure 32. Cell seeding completed animation still
26	Figure 33. Streamlined CMF reconstruction animation still
30	Figure 34. Angiogenesis screenshot
31	Figure 35. Angiogenesis visualization depending on selection

<b>Page</b>	<b>Table</b>
18	Table 1. Angiogenesis over time (days)



# INTRODUCTION

## **Background**

### *Bone grafts*

Currently, the process of organ and bone organ transplant is classified into autografts, allografts, xenografts, synthetic materials, or any combination thereof (Elsalanty 2009). An allograft is a same-species transplant, while a xenograft is a transplant from one species into a different species. For instance, a modern day example of a xenograft would include the implantation of a decellularized pig lung scaffold into a human.

The most common surgical reconstruction of large craniofacial defects consists of a bone graft classified as an autograft, the transfer of bone from one site to another within a single patient. Here, a typical donor site will be sourced from the iliac crest, calvarium, ribs, or olecranon (Singh 2011).

Traditional bone grafts have many constraints and complications, including a limited amount of bone that can be transferred, high donor site bone tissue morbidity, and the task of aesthetically matching a complex facial structure at the site of defect. In addition, the graft itself must be highly vascularized, and the healing process must be monitored for graft incorporation, mechanical stability, and restoration of function (Elsalanty 2009).

### *Biomaterials*

The newest advances in 3D-printing biomaterials foresee a vastly improved surgical procedure that would allow the surgeon to graft a 3D-printed scaffold perfectly shaped to fit the patient. The scaffolds themselves are generated from the patient's CT scans and printed using Fused Deposition Manufacturing (FDM) printing technology

in polycaprolactone (PCL), a material commonly used as reabsorbable suture material. The concept then combines research on adipose-derived stem cell assemblies, osteo-inductive cues, and oxygen microtank technology, into a streamlined surgical approach to reconstruct craniofacial defects (Temple 2014).

### **Problem Statement**

The progress of vascularized craniofacial bone regeneration has been hampered due to the lack of visuals explaining 3D-printed craniofacial scaffolding and the complex science behind its success. The preceptor for this research could not identify appropriate visualizations to teach the clinical process from CT scan, to surgical implantation, to bone regeneration, and therefore this research project represents the first of such visualizations. A literature review was conducted to confirm that there were no existing animations.

### **Objectives**

The visualizations produced as part of this research will fulfill the lack of storytelling visualizations for vascularized craniofacial bone regeneration with the creation of (i) entirely novel presentation visuals/animations of 3D-printed craniofacial scaffolding methods, and (ii) a browser-based interactive presentation of simulated bone scaffold angiogenesis. Moreover, the principles and findings taught through these presentations can be applied to other areas of medical research, such as sites besides the craniofacial region or general bone angiogenesis technique.

The animations covering craniofacial scaffolding will have a didactic structure of 5 key points as follows:

- I. An anatomically-shaped graft is essential for functional craniofacial bone regeneration.

- II. The composition of the 3D-printed scaffold before implantation.
- III. The regeneration process from 3D-printed scaffold to organic bone tissue.
- IV. The workflow from CT scan to operation.

From the browser-based 3-dimensional angiogenesis simulation, the audience will understand:

- V. The pathway and cell assembly during angiogenesis.

The innovative aspects of this research includes the first creation of presentation visuals/animations of 3D-printed craniofacial scaffolding methods, with a scientifically and visually accurate depiction of the scaffold at high microscopic power, and the steps of angiogenesis. In addition, the research documents optimized approaches to visualizations of common biological processes using Cinema 4D (MAXON, Friedrichsdorf, Germany), including the use of alpha channel texture on modeling cells, animation of the “3D printed” scaffold, and a streamlined approach for manipulating cell movement to depict angiogenesis.

## **Audience**

The resulting visualizations will be aimed at three groups of audiences: (i) patients, (ii) plastic/reconstructive surgeons, and (iii) biomaterials scientists. For patients, it is important to understand the process and timing of the major surgery they will undergo, as well as what to expect during post-operative recovery. Surgeons will become familiar with the surgical implant pipeline for later use in practice, as well as the medical science behind treating their patient for reconstructive craniofacial surgery. Finally, for biomaterials scientists, the scaffolding and biological mechanisms will be relevant to understanding the current state of research. There will be three iterations of the animated sequences with different levels of information, such that the presenter can adjust to the

# MATERIALS AND METHODS

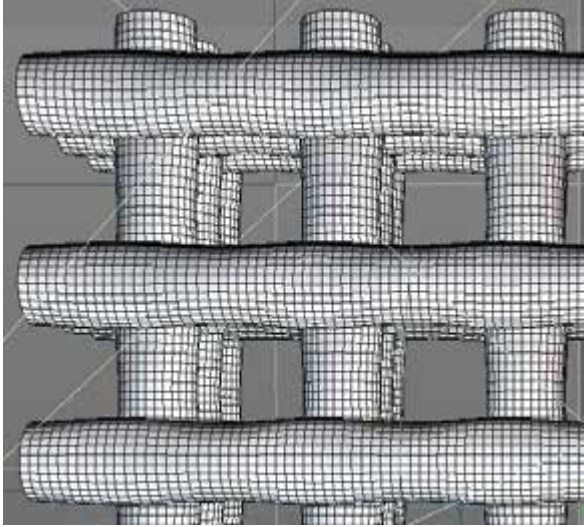
## **Overview**

A literature review was initially conducted on bone grafts, 3D-printed scaffolds, and adipose-derived stem cells. A 3D-printed scaffolding lab and its angiogenesis research were observed to ensure an accurate depiction of methods and tools used. This information was organized such that it captures the main objectives and narrative elements. Illustration and animation assets were created digitally using a combination of Photoshop® (Adobe® Systems Inc., San Jose, California), ZBrush® (Pixologic, Los Angeles, California), and Cinema 4D™ (Maxon, Friedrichsdorf, Germany). Narration was recorded and saved using Audacity® (The Audacity Team, Pittsburgh, Pennsylvania) and Audition® (Adobe® Systems Inc., San Jose, California). After Effects® (Adobe® Systems Inc., San Jose, California) was used for final compilation and rendering of the animations.

The angiogenesis interactive simulation is browser-based, with visual elements created using ZBrush and Cinema 4D, and the animation was made using Cinema 4D. The final interactive animation was coded using HTML and Javascript. This simulation will be an accurate interactive visualization of the key steps, and will be based on previously published data on scaffold angiogenesis (Hutton 2012).

## **Scaffold Contents: Setting and Scale**

According to the literature, the scaffold properties that best support seeded human stromal-vascular fraction cells have an infill PCL density of 40%, approximated with PCL struts of 0.5 mm in diameter with a pore size of 0.8 mm (Temple 2014). Within these scaffolds can be the incorporation of oxygen microtanks, with a diameter of an average of 75  $\mu\text{m}$  (Cook 2015).



**Figure 1: Porous scaffold modeled in Cinema 4D with an infill PCL density of 40%.**

The scaffold can also be seeded with stromal-vascular fraction cells (aka. adipose-derived mesenchymal stem cells), which range an average of 17-30  $\mu\text{m}$  in diameter (Ge 2007). The cells are put into the pores of the scaffold in combination with a fibrin gel that contains fibers of up to 900nm in diameter (Ariens 2013). Given the drastic size difference between the

scaffold struts and its contents, the stromal-vascular fraction cells and fibrin diameters were exaggerated in the conceptualizations produced as part of this research for visual clarity. In addition, the density of cells in the scaffold matrix was lowered for the audience to have a holistic overview of scaffold contents.

## **Narration**

The narration utilized technical science terms, followed by definitions for the lay audience. A “storytelling” approach was taken to best communicate the objectives of craniofacial scaffolding, its biological and synthetic contents, and steps used in a clinical setting.

The narration was recorded and edited with the generous help of Alex Rosensweet using the program Audacity® 2.1.2, an audio freeware application available online. The microphone/recorder was a H4n ZOOM (Zoom® Corp., Tokyo, Japan) attached to a regular microphone stand with a pop filter, and adjusted to a 90 degree pickup.

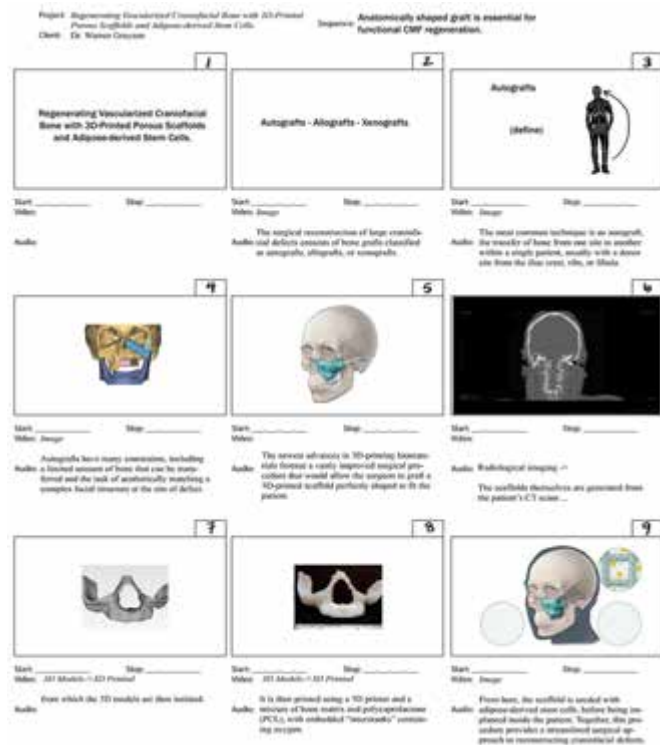
Markers were set using Audition® to denote key phrases to which animation keys could be matched (**Fig. 2**).



**Figure 2: Screenshot of narration file with markers in Audition®. Text is not intended to be read.**

## Storyboards

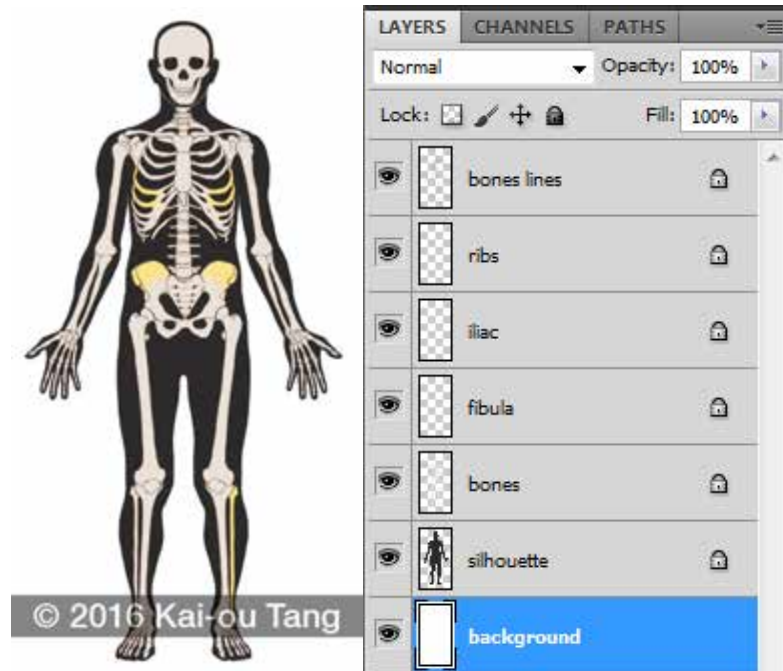
The storyboards were created using Photoshop (Adobe® Systems Inc., San Jose, California), using image frames sized in a 16:9 aspect ratio, with 6 frames per page. Each frame was paired with its respective audio narrative (**See Appendix D-G**).



**Figure 3: Storyboards for Part I: Anatomically Shaped Graft is Essential for Functional CMF Regeneration. Text is not intended to be read.**

## Asset Creation (2D Visual Elements)

The two-dimensional visual assets were created using Photoshop, with layers organized with the final animation in mind. These assets include a silhouette and skeleton, pipetting figure, face silhouette, and icons for animation objective IV.



**Figure 4A and B: A. Image of the silhouette and skeleton PSD file. B. A screenshot of the silhouette and skeleton layers in Photoshop.**

## CT Scan Sequence

Images used to represent the CT scan were constructed using the MANIX OsiriX MD TM model (Pixmeo SARL®, Geneva, Switzerland), and exported using the OsiriX 2D renderer function.

These would later be used in an animated sequence to describe the reconstruction of DICOM datasets into a 3D model (**Fig 5**).



**Figure 5: OsiriX Manix DICOM dataset used to export a series of 2D images for later incorporation into animated sequence.**

## Asset Creation of 3D Models

Three-dimensional assets were modeled using a combination of OsiriX MD, ZBrush, and Cinema 4D. Images were test rendered as 800x600 PNG clip files to check for lighting and texture before the final render.

### *Skull*

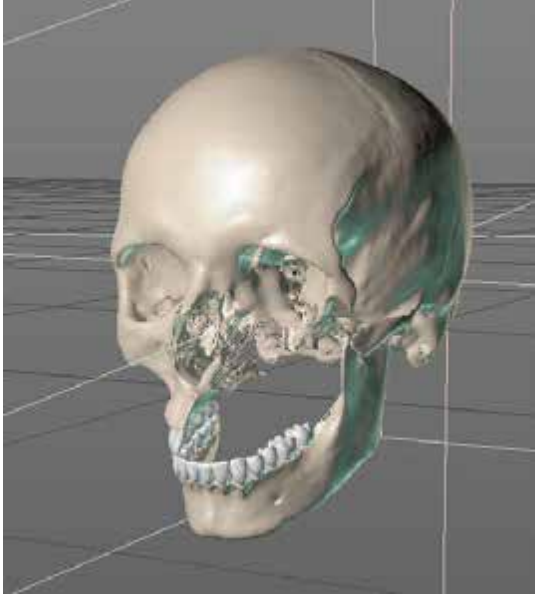
The main skull 3D model was extracted from CT scans using OsiriX MD. CT scan datasets with file names MANIX and MELANIX were acquired from the OsiriX site (DICOM Sample Image Sets, 2014), each containing the cranium and mandible of separate skull CT scans. The bone structures were isolated using Osirix 3D Surface Rendering and 3D Volume rendering functions and exported at a high resolution as OBJ files. The models were then cleaned of debris data using a combination of Meshlab TM (ISTI-CNR Research Center , Pisa Italy) and ZBrush. Finally, the two cranium and mandible models were combined into one complete skull 3D model using ZBrush (**Fig. 6**).



**Figure 6: Finalized skull 3D model in ZBrush. Later to be exported as an OBJ file.**

The cranium and mandible were separated from one another as individual ZBrush subtools using ZBrush's Split Groups function. The teeth were further separated from both the cranium and mandible subtools. This was done so the teeth could not only be textured separately, but also because the presence and removal of teeth were notable components in key parts of the animation.

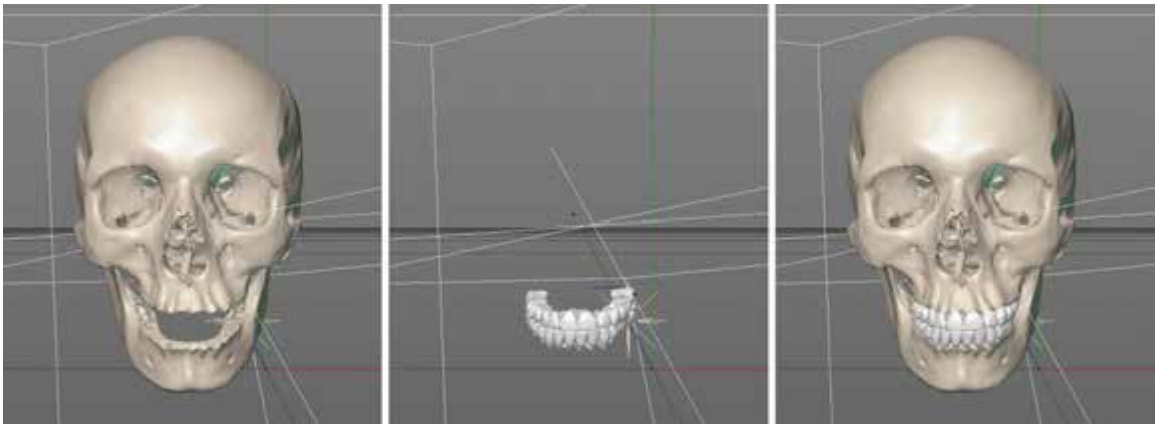




**Figure 7: “Injured” skull model in Cinema 4D. Both the full and injured skull and teeth models were exported from ZBrush as .OBJ files and were imported and textured using Cinema 4D.**

An injured cranium version was created using ZBrush based on surgical information provided by Drs. Amir Dorafshar and Warren Grayson. A 2D separate image graphic was also created and saved as a JPEG file, since a skull injury is often used within Dr. Grayson’s presentations. Creation of the injury was done by modifying the original skull using Selection Brushes and Delete Hidden commands in ZBrush. Recreation of an injured cranium served the dual purpose of being edited for audience

clarity, and to protect patient information that may have been apparent if a single original CT scan (Fig. 7).



**Figure 8: Final skull and teeth models, textured separately in Cinema 4D.**

### *Three Dimensionally Printed Scaffold*

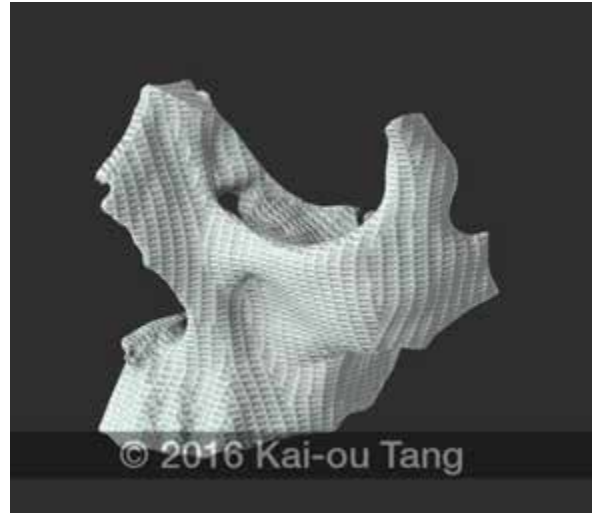
The scaffold was created in ZBrush by hiding and deleting parts of the original skull 3D model. A section including part of the orbit, zygomatic arch, nasal and maxillary

region was chosen to best illustrate the complexity of a craniofacial structure. It was then exported from ZBrush as an .OBJ file and imported into Cinema 4D for texturing.

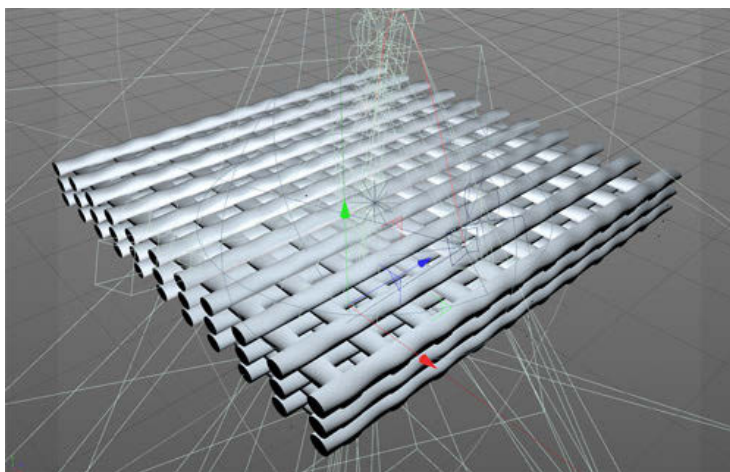
To recreate an actual 3D printed scaffold with qualities of a printed porous grid, a combination of **Cinema 4D Materials Editor>Channels>Color and Bump** were used along with a Brick

texture setting. This resulted in a gridded porous-like texture while keeping the three dimensionality of the scaffold that is optimized for animation (**Fig. 9**).

For the animation sequence in Part I that communicates the illusion of “printing a scaffold”, a Boole function was used in Cinema 4D. This is further addressed as part of the *Optimized Approaches to Biovisualization (Using Cinema 4D)* section.



**Figure 9:** Model of the 3D-printed scaffold, textured in Cinema 4D and intended to fit over “injured” skull.



**Figure 10:** Entire model of the 3D printed porous scaffold with lighting in Cinema 4D.

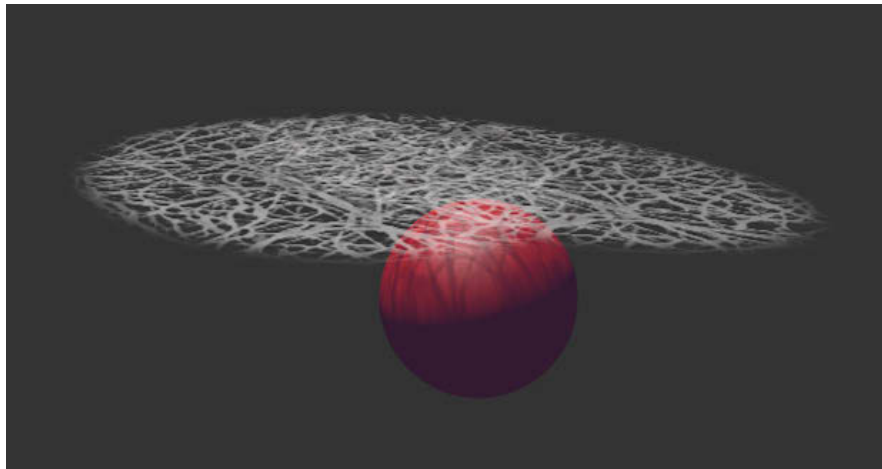
### *Microscopic Scaffold*

The microscopic view of the scaffold was created using the Loft Deformer function in Cinema 4D using geometry created of a single 3D printed strut. The strut was multiplied and arranged in a grid shape according to

the aforementioned measurements. For visualization purposes, a 10 x 11 x 3 strut grid was created such that the 3D scene camera could pan across it (**Fig. 10**).

### *Fibrin*

The fibrin model was created in Cinema 4D using a Plane Polygon, Displacer Deformer for variation, and an Alpha Channel, to which a black and white photograph of fibrin was applied. A test was performed to confirm whether the fibrin visualization would cast a shadow as a plane or as a result of the alpha channel details (**Fig. 11**). The latter proved to be the case.



**Figure 11: Fibrin alpha channel lighting test. Note detail of shadow cast as a result of the alpha channel image of fibrin.**

### *Oxygen Microtanks*

The oxygen microtanks were created in Cinema 4D to visualize oxygen (red spheres) releasing and permeating through the microtank.

To do this, a single sphere was modeled with another placed into it using the Boole function. The red oxygen spheres were made to fill the area using a Cloner function with a Volume setting. A Rigid Body tag was added to the red oxygen spheres such that when the footage was played, they would dissipate outwards through the walls of the microtank (**Fig 12.**).

Since there is a dense population of microtanks within the scaffold PCL, this visualization was then duplicated using AfterEffects. A mockup of the layout of the oxygen microtanks was created in Cinema4D for placement purposes using the Cloner function (Fig. 13).



Figure 12: Animated renders of oxygen (red spheres) being released from the microtanks.

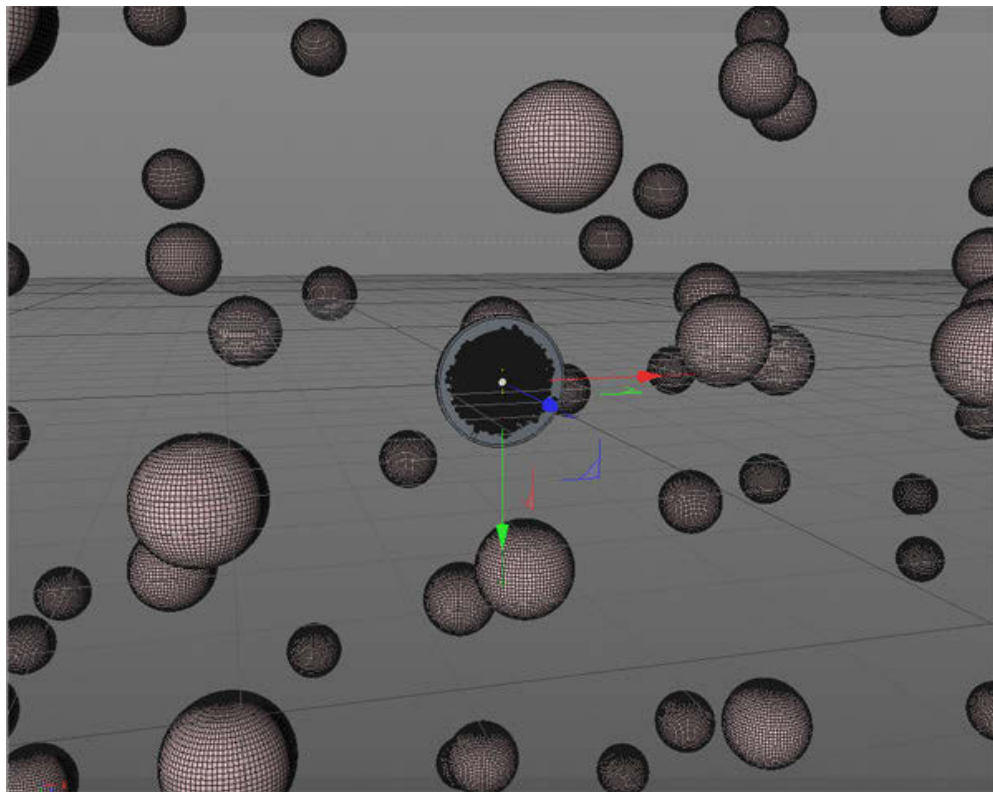


Figure 13: Layout mockup of the oxygen microtanks in PCL using Cinema 4D.

## Optimized Approaches to Biovisualization (using Cinema 4D)

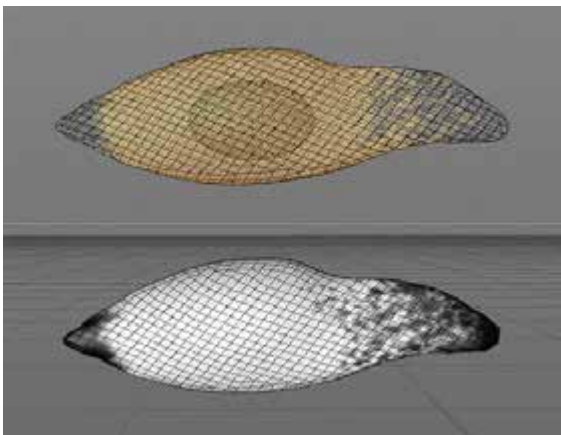
### *Adipose-derived stem cells*

Polygon optimization was key for the adipose-derived stem cells, as they would be used in a scene where there were over 600 moving cell instances. Thus, in lieu of modeling the “fibrous texture” of the extracellular adhesion matrix proteins (which would greatly increase the polygon count), an alpha channel texture was used such that parts of the cell were transparent with a fibrous appearance.

A UV map was assigned to the stem cell model in Cinema 4D before unwrapping the UV map and exporting it into Photoshop. In alpha channels, white areas are rendered opaque while black is rendered as transparent. Thus, the fibrous areas of the cell were painted black, shown in Figure 14.



**Figure 14: The UV map for the adipose-derived stem cell. Here, the grid-like structures represent the model polygons. Most of the map is white (opaque), while black texture is painted where the cell will be transparent.**

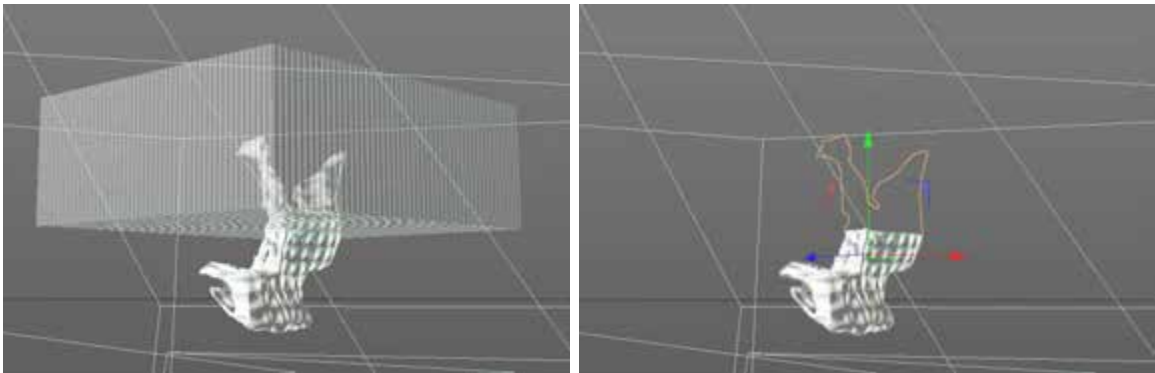


**Figure 15: Adipose-derived stem cell with UV map assigned on color layer (top) and re-imported into alpha channel (bottom).**

The new UV map was re-imported into Cinema 4D’s Materials editor in the Alpha Channel option. These cells were then color coded red to represent vascular progenitor cells, and a pale white for bone progenitor cells.

### *“Printing” the Scaffold*

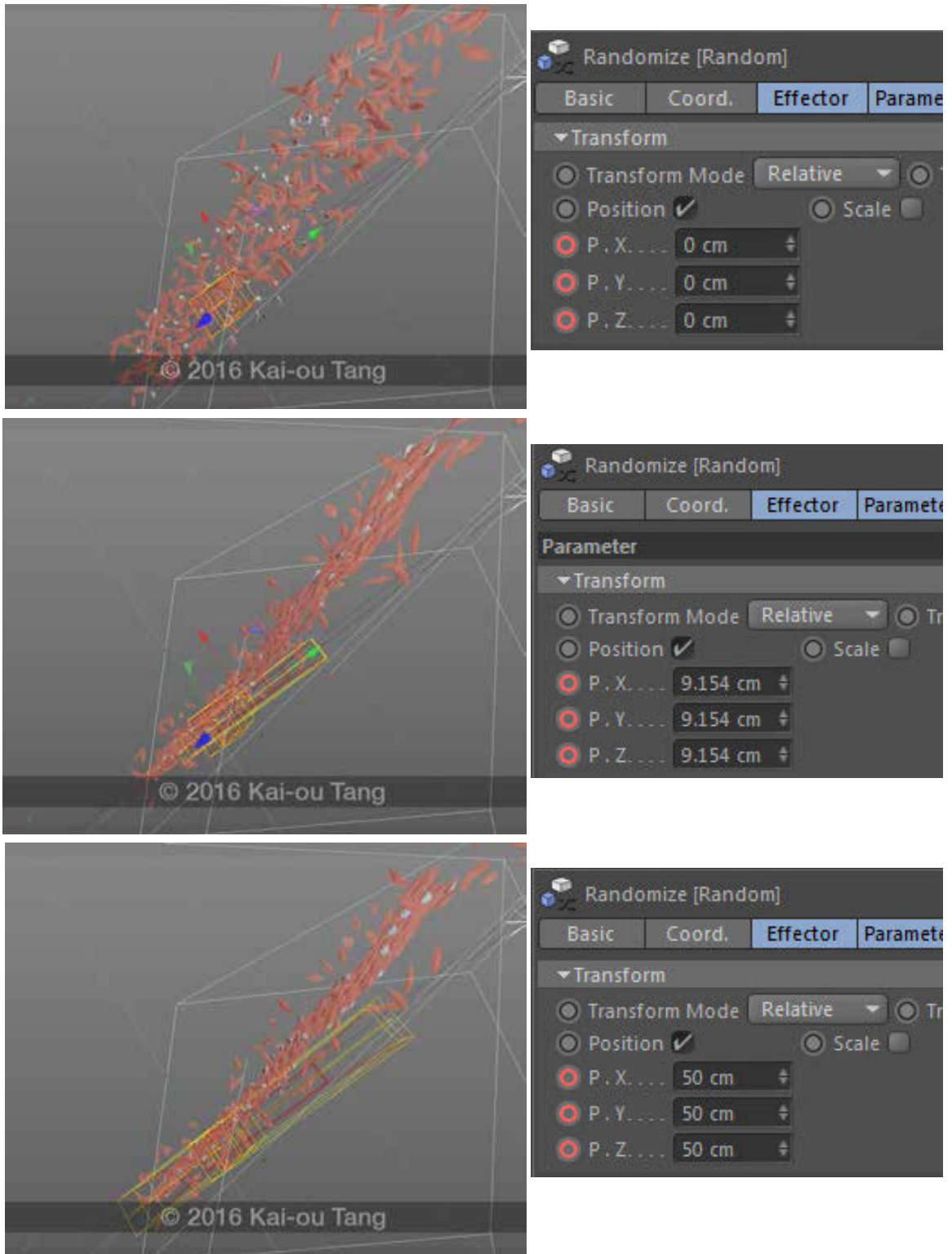
To create the illusion of the scaffold being 3D printed in Part I, a cube was keyframed first entirely overlapping the scaffold, then moved upwards until it was completely above the scaffold. The cube and scaffold model were then placed inside the Boole function, both with the same texture such that the final visual would appear like a uniformly textured object.



**Figure 16A and B: A: Before the Boole is applied, the cube is visible and overlapping the scaffold model. B: After the Boole is applied, the cube area is subtracted from that of the scaffold.**

### *Angiogenesis*

In order to retain an organic shape to the vessel, not only was a Cloner function used with Rendered Instances checked, but an additional Fracture function was placed inside of this. With Fracture, the cells could be arranged with variable distribution across the diameter, in addition to the pericytes being placed outside the perimeter of the vascular progenitor cells. In order to get the cells to “organize”, a Random effector was added to the Cloner with the Position keyframed, first with a starting value of 50cm, then decreased to 0cm over a span of 300 frames (see Fig 17A, B, and C below).



**Figure 17A, B and C: Progress of angiogenesis animation as correlated to the Random effector. On the left is the Cinema 4D viewport, on the right is the window of the Random effector. Note that the values for Random effector Position decrease over time.**

**A: Angiogenesis at 0 seconds, B: Angiogenesis at 10 seconds, C: Angiogenesis complete at 16 seconds.**

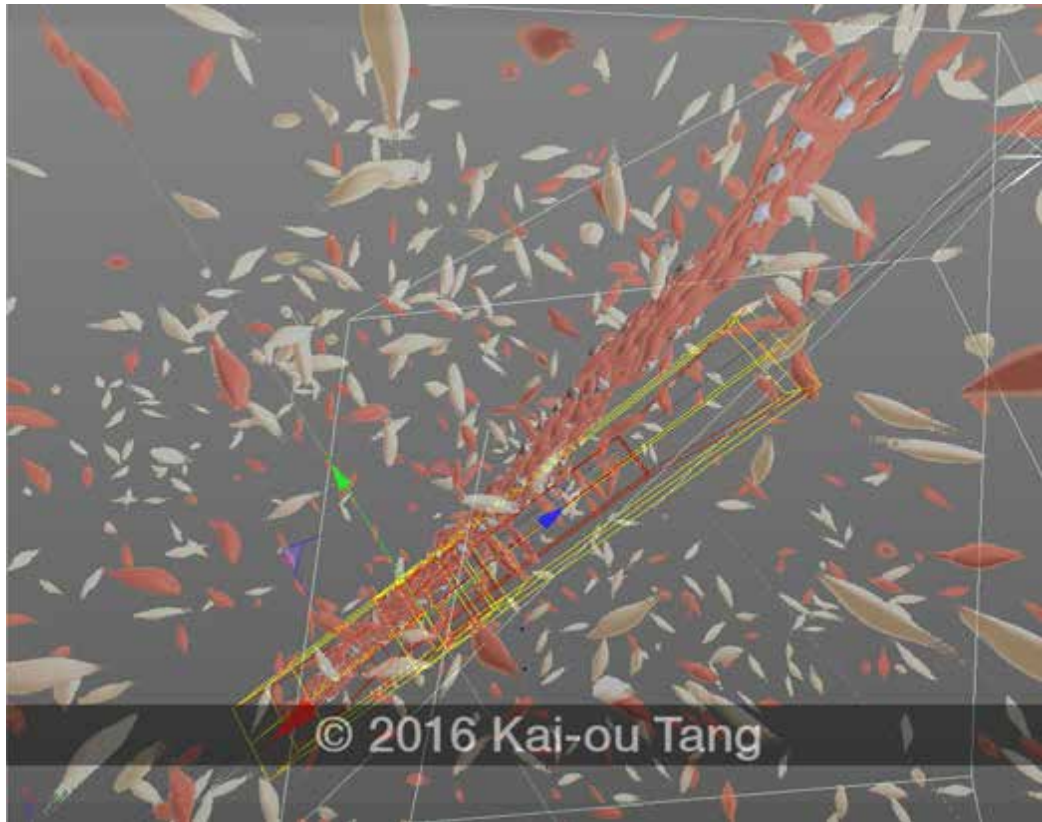


Figure 18: Final layout of angiogenesis with additional bone progenitor cells.

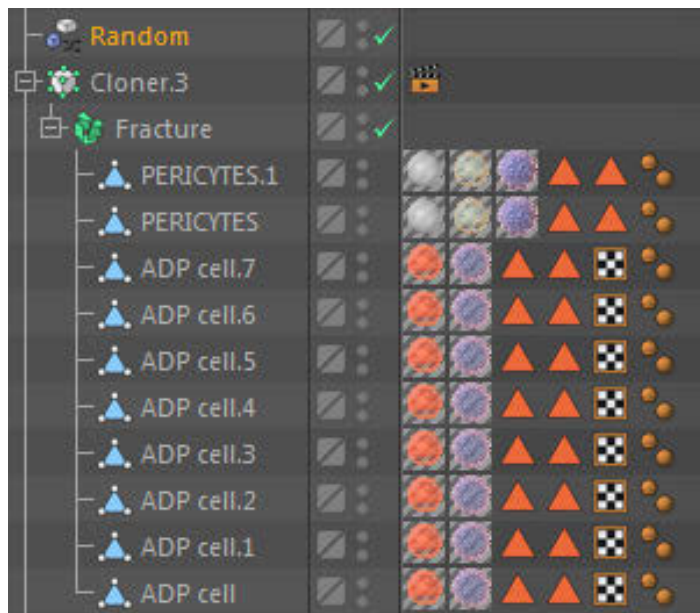


Figure 19: Angiogenesis models as viewed in the object manager. Note the Fracture effector within the Cloner effector (here, labeled “Cloner.3”). This allows for manual rearrangement of the models in 3D space.



### **3D Animation**

For the animated sequence of Part I, final clips were rendered in Cinema 4D as a series of 1800 x 1350px PNG clip files, with a transparent background for overlay. The 3D models were optimized for render speed by reducing polygon count and lighting without the use of Ambient Occlusion. Since the project required a render time of more than 30 minutes per frame, and the chosen animation frame rate was 30.0 frames per second, more complex 3D rendering would have easily been detrimental to the progress of the thesis. The animation clips were separated and rendered by scenes, such that there were 14 clips total.

### **Compositing and Final Rendering**

The 2D and 3D assets for parts I and V were composited using AfterEffects. The 2D assets were imported as PSD files, and the 3D animations imported as PNG clips. The narration was imported as an Auditions AIFF file, such that markers remained intact, and could be lined up with the animation.

The final movie file was rendered using AfterEffects as an .AVI file and converted to an .MP4 file using Media Encoder® (Adobe® Systems Inc., San Jose, California).

### **Angiogenesis Interactive Presentation**

The premise for the angiogenesis interactive presentation was for the user to interact with the webpage and learn the effect that oxygen level has on the timeline of angiogenesis. Here, the two mutually exclusive oxygen concentration options are “Normoxia (20% Oxygen)” and “Hypoxia (2% Oxygen)”. As the angiogenesis MP4 plays, and a timeline description would be displayed below that reads “Angiogenesis at \_\_ days,” corresponding to both the animation time, and the level of oxygen that the user selects.

The coding for the webpage was created in Notepad with a combination of HTML, Javascript, paired with the final MP4 render mentioned previously. First, the MP4 file was uploaded and placed into the browser page.

```
<div id="stage" style="text-align:center">
  <video src="http://www.kaioutang.com/img/angio_micro.mp4"
  id="video1" width="800" muted="muted" controls></video>
</div>
```

**Figure 20: HTML for angiogenesis MP4 file in browser page.**

Next, the “Angiogenesis at \_\_ days” coding was scripted with Javascript. The correlation of angiogenesis during Normoxia to Hypoxia is a vessel length of 5:6 (Hutton, 2012). That is, the vessel length at Day 12 under Normoxia is approximate to Day 14 under Hypoxic conditions. Because the angiogenesis animation itself spans 16.9 seconds, after converting seconds to days, a ratio of  $x = 0.829$  of the timeline was determined for Normoxic conditions, and  $x = 0.966$  for Hypoxic conditions (“Radio Button Onclick vs. Onchange Event”, 2001).

	Animation timeline				
	0.0 sec	4.2 sec	8.5 sec	12.7 sec	16.9 sec
<b>Normoxia (*0.829 of Animation timeline)</b>	0.0 days	3.5 days	7.0 days	10.5 days	14.0 days
<b>Hypoxia (*1.021 of Animation timeline)</b>	0.0 days	4.1 days	8.2 days	12.2 days	16.3 days

**Table 1: Angiogenesis over time (days) as it correlates to the MP4 Animation.**

In terms of coding, this was achieved as Javascript coding that updates and replaces the label “Angiogenesis at \_\_ days” based on whether Normoxia or Hypoxia is selected. The selection of Normoxia vs Hypoxia changes the ratio by which the video timeline is multiplied (also known as var x) (Lawson, 2010).

```
<div id="time" style="text-align:center; color:#f2664a; font-weight:bold; font-size:32px;">Angiogenesis at 0.0 days</div>
```

**Figure 21: Label text with HTML so that “Angiogenesis at 0.0 days” updates alongside the video.**

```

<form action="#" method="post" class="Form" id="oxySelect">
<div style="text-align:center; color:white; font-weight:bold;
font-size:20px;">
    <label><input type="radio" name="group1" value="0.829"
checked /> Normoxia (20% Oxygen)</label><br>
    <label><input type="radio" name="group1" value="0.966" />
Hypoxia (2% Oxygen)</label><br>
</div>
</form>

```

**Figure 22: HTML coding allowing for radio button selection of either “Normoxia” or “Hypoxia” with a rate of 0.829 and 0.966, respectively.**

```

<script type="text/javascript">
(function(){
    var v = document.getElementsByTagName('video')[0]
    var t = document.getElementById('time');
    var x = 0.829;

    // Oxygen level onclick
    var group1 = document.forms['oxySelect'].
elements['group1'];

    for (var i=0, len=group1.length; i<len; i++) {
        group1[i].onclick = function() {
            x=this.value;
            t.innerHTML = ' Angiogenesis at ' + parseFloat(v.
currentTime*x).toFixed(1) + ' days ' ;
        };
    }

    for (var i=0, len=document.forms.length; i<len; i++) {
        document.forms[i].onsubmit = function() { return
false; };
    }

    v.addEventListener('timeupdate',function(event){
        t.innerHTML = ' Angiogenesis at ' + parseFloat(v.
currentTime*x).toFixed(1) + ' days '
    },false);
})();
</script>
</div>

```

**Figure 23: Javascript coding for the “Angiogenesis at 0.0 days” to update depending on whether “Normoxia” or “Hypoxia” is selected, as well as the time of the video.**

Instructional text, which read “Move the video slider left and right to see how oxygen levels affect vessel growth time (days)” was added via HTML. Text regarding the source of the supporting journal article, “Hutton DL, Logsdon EA, Moore EM, Gabhann FM, Gimble JM, Grayson WL. Vascular morphogenesis of adipose-derived stem cells is mediated by heterotypic cell-cell interactions. *Tissue Engineering Part A*. 2012; 18:1729-1740,” was also added to the bottom of the page. Afterwards the HTML page was tested for functionality before being uploaded online. Refer to Appendix C for the completed and compiled version of the HTML and Javascript coding used in the Angiogenesis interactive presentation.

## RESULTS AND DISCUSSION

### Goals

To fill the current absence of visual media for vascularized 3D-printed craniofacial bone regeneration, all key points of the research identified bellows as I through V were storyboarded (see Appendix D-G). Part (I) “An anatomically-shaped graft is essential for functional craniofacial bone regeneration” was animated and exported for distribution as an MPG4 movie file. Part (V) “The pathway and cell assembly during angiogenesis” was animated and assembled as an html interactive presentation that can be accessed online.

### **Part I: An Anatomically-Shaped Graft is Essential for Functional Craniofacial Bone Regeneration.**

The first part of the animation introduces the concept that an anatomically-shaped graft is essential for craniofacial bone regeneration. Backgrounds are kept solid and unobtrusive throughout the animation, such that it is not distracting to the audience and they are able to absorb and focus on the on-screen information. In addition, the background color was used to convey atmosphere, with a desaturated dark palette for the current methods of grafting bone, and a brighter blue tone when the newer 3D-printing



**Figure 24: Animation still visualizing the complexity of craniofacial structure, next to different classifications of bone grafts.**

scaffold is introduced. An injured model is presented to the audience, with a polygonal overlay highlighting the complexity of the craniofacial topology. Next, the current types of bone grafts are identified as autograft, allograft, and xenograft (**Fig. 24**).

As the autograft is most common, it is defined and used as an example to teach the pros and cons of current surgical standard bone grafts. This sequence familiarizes the lay audience to the constraints of bone grafting, while reminding surgeons and biomaterials scientists the reasons for innovating a different type of grafting process.



**Figure 25: Animation still defining autograft and areas of skeleton from which bone grafts are most frequently sourced.**



**Figure 26: Animation still explaining the constraints of autografts. The right side is a visualization of current methods of an autograft planning orientation of fibula grafts onto the skull.**

The next sequence introduces Dr. Warren Grayson’s concept and work: A 3D-printed scaffold custom-shaped to fit the patient. The scaffold is depicted filling in a complex area of the skull, such that the audience gets the full impact and importance of an anatomically shaped graft. The scaffold is depicted with a porous opaque texture.

During the animating process, the topic of whether “teeth” should be included came up. In the clinical setting, teeth would not be a part of the scaffold, and would have to be implanted later in the procedure. After consulting the subject matter expert, Dr. Warren Grayson, it was determined that the focus would be on the scaffold, and the presence of teeth may raise more questions than otherwise. Therefore as to not confuse the audience, it was decided that they should not be included in the sequence.



**Figure 27: Animation still where the 3D printed scaffold is grafted onto the injured skull. Note the brighter, more saturated background color to emphasize the new and promising technology.**

The animation then explains and visualizes the process of constructing the scaffold. For the benefit of the audience, the process is divided into 5 steps: Radiological imaging (CT scan acquisition) > 3D Models (reconstructed from CT datasets) > 3D

Printed > Seeded with cells > Surgical implantation. The transitions between these 5 steps were vital as a process sequence, to best instruct the audience on the linear yet interconnected nature of scaffold creation. It also emphasizes a patient-centered approach, as the viewer observes that the process starts from the patient's own CT scans, and is customized specifically to their injury and craniofacial structure.

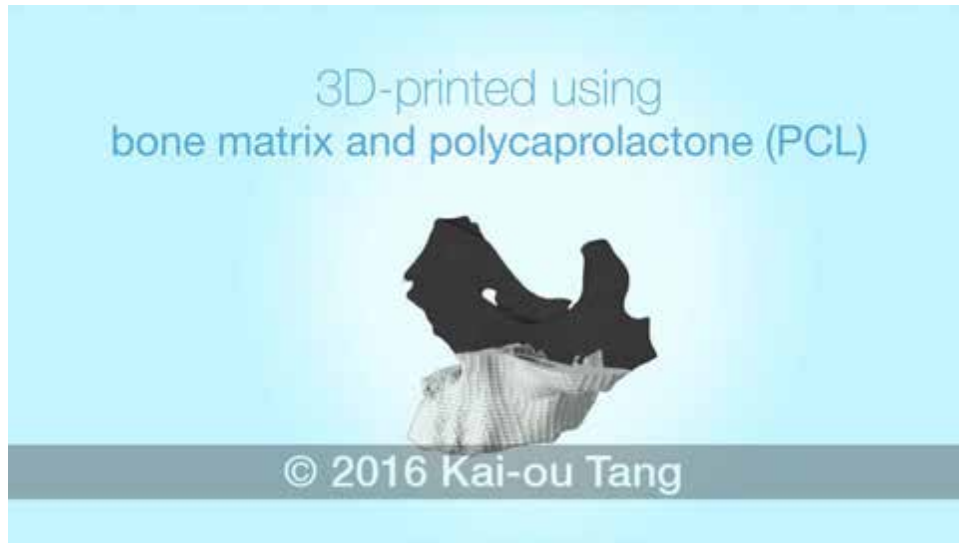


**Figure 28:** Animation still depicting the 3D model being extracted from patient CT data. Text is not intended to be read.



**Figure 29:** Animation still where the gray skull represents 3D model data extracted from CT scans, and the purple model represents isolated and mirror-imaged anatomy, from which the scaffold will be printed.





**Figure 30:** Animation still depicting the 3D printed scaffold based on the mirror-imaged 3D model.

The final sequence of Part I provides a preview of the science behind a biologically regenerated 3D-printed scaffold. Because this visualization intends to introduce the audience to the science, explanations are simplified, and will be further detailed in Parts II-IV. First is an animation of the operator pipetting “Stromal-fraction cells” onto a “Porous scaffold”, followed by a callout label for stromal-vascular fraction cells fading out and reappearing within the porous scaffold label (**Fig. 31-32**). Stromal-vascular cells



**Figure 31:** Animation still where the operator is pipetting stromal-vascular fraction cells and fibrin into the porous scaffold. Text is not intended to be read.

are colorized yellow so when they are later identified as adipose-derived stem cells, it will reinforce the association. The label, operator, and pipette disappear, and the seeded scaffold is finally implanted into a skull within a silhouette of a human head (**Fig. 33**).



**Figure 32: Animation still depicting stromal-vascular fraction cells and fibrin within the porous scaffold.**



**Figure 33: Concluding animation still depicting the scaffold grafted onto the injured skull, within the patient's silhouette.**

## **Part II: The 3D-Printed Scaffold Before Implantation.**

Part II details the scientific process through which scaffold components lead to biological regeneration. It divides the elements into (1) Oxygen microtanks, (2) Bone matrix cues, and (3) Adipose-derived stem cells. This segment is critical to viewers who would ask for the scientific theories behind the viability of bone regeneration. First, an overview is given regarding the scaffold, which is 3D printed as a mixture of polycaprolactone (PCL), bone matrix cues, and oxygen microtanks. Bone matrix cues are specifically calcium phosphate, but pathways of mineral deposition are not detailed here, as the focus is on the scaffold itself. The storyboard then details oxygen microtanks, providing a visualization of the release of oxygen through gas permeable microscopic hollow balloons, as well as its density within the PCL. Finally, details of adipose-derived stem cells are provided. An explanation is given of its acquisition through lipoaspiration, as well as traits that make it best suitable for biological regeneration after surgical implantation.

## **Part III: The Regeneration Process from 3D-printed Scaffold to Organic Bone Tissue.**

Part III teaches the biological process of bone regeneration as the 3D-printed scaffold degrades after implantation. Due to time constraints, these sequences were storyboarded and not animated, though the elements of biocommunication and animation would parallel to those identified in Part I. The course of regeneration is divided into 6 steps as follows:

1. *A pre-fabricated, biodegradable, porous scaffold provides structure to guide the shape of bone tissue regeneration.* Here, the anatomically-shaped scaffold is reintroduced with labels highlighting its porous grid-like composition, and oxygen microtanks embedded within the PCL.
2. *Extracted adipose-derived stem cells are placed into a pre-fabricated scaffold*

*and immediately transplanted to the bone defect site.* Stromal-vascular fraction cells are identified as analogous to adipose-derived stem cells.

The site of extraction (through lipoaspiration), is illustrated briefly but not expounded on, as adipose-derived stem cells are detailed in Part III.

3. *Controlled delivery of oxygen from the scaffold supports stem cell survival through use of oxygen microtanks.* A holistic view of the scaffold containing adipose-derived stem cells, fibrin, and oxygen tanks are shown and labeled before the scaffold is implanted into the patient. This emphasizes the “initial” biological status of the scaffold upon surgical implantation.
4. *Newly-formed blood vessels developed from transplanted stem cells connect with existing blood vessels from neighboring tissues to provide a continuous blood supply.* Vascular generation is essential to biological regeneration, so it is emphasized as its own step. Scaffold contents differentiate from adipose-derived stem cells to form vascular progenitor cells, in this case, simplified into homogenous epithelial cells. They self-assemble into vessel structures and connect to the patient’s existing vessels.
5. *Fat stem cells differentiate into bone forming cells and deposit new mineral to fill scaffold pore spaces.* Alongside vascular progenitor cells, adipose-derived stem cells also differentiate into bone progenitor cells (osteoblasts). Both vascular and osteo progenitor cell components make up the majority of biological regeneration during scaffold degradation.
6. *The 3D printed scaffold degrades leaving only a biological bone replacement that responds to physiological signals.* A concluding visualization is presented of scaffold degradation being replaced by vascular and osteo progenitor cells identified in Steps 4 and 5.

#### **Part IV: The Workflow from CT Scan to Operation.**

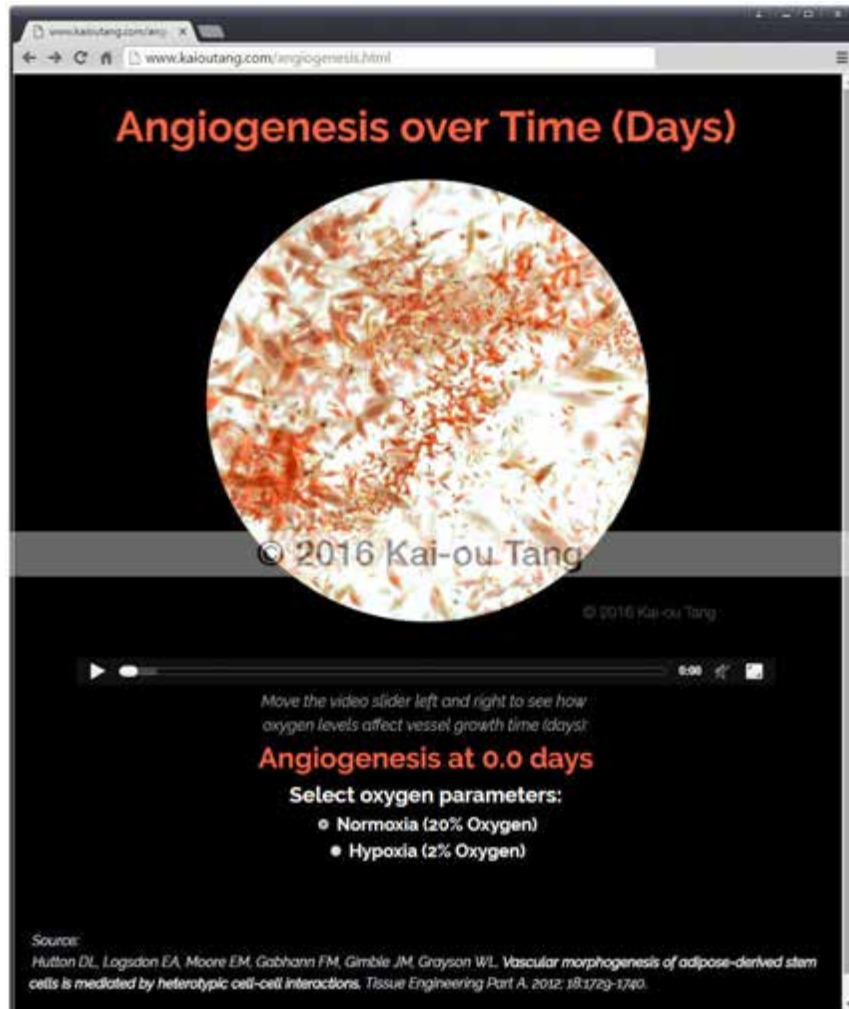
The concluding part of the animation aimed to give an all-encompassing overview of the clinical procedure, while emphasizing the purposefully concentrated timeline from diagnoses to surgical implantation. Building on the previously presented information, the clinical steps were broken down into 5 steps:

1. CT scans are taken of the patient.
2. An anatomically-shaped 3D model is created of the missing bony anatomy.
3. The 3D model is then 3D-printed into a scaffold, which is then packaged and sent to the operating room.
4. The surgeon adds lipoaspirated adipose-derived stem cells to the scaffold in a sterile environment,
5. The processed scaffold is surgically implanted into the patient.

Though some of the steps are visited in earlier parts of the animation, this section aims to provide a memorable summary of the entire process, while also adding the sterile processing and surgical implantation components of the procedure.

#### **Part V: Angiogenesis Interactive Presentation**

The process of angiogenesis is presented in a browser format, such that it is easily accessible online to both the lay audience and scientists, without the need for file distribution or download. Because it is coded using HTML and Javascript, no additional software or plugins are necessary. The main visualization is a 16.9 second 3D animation of cell assembly during angiogenesis. At the top of the page is the title of the interactive presentation, “Angiogenesis over Time (Days)”. Below the MP4 file are instructions on how to use the video slider control that read, “Move the video slider left and right to see how oxygen levels affect vessel growth time (days):”. Underneath this is a timeline



**Figure 34: Screenshot of the browser-based angiogenesis interactive presentation. Text is not intended to be read.**

statement that reads, “Angiogenesis at 0.0 days,” followed by two radio buttons labeled “Normoxia (20% Oxygen)” and “Hypoxia (2% Oxygen)”.

If the user presses play right away, Normoxia is selected by default, and the “Angiogenesis at \_\_\_ days” will start at from “Angiogenesis at 0.0 days”, increase linearly, and end at “Angiogenesis at 14.0 days”. The user may at any time pause the video, or select the “Hypoxia (2% Oxygen)” radio button, which will convert the “Angiogenesis at \_\_\_ days” statement to the number of days under Hypoxic conditions. In addition, if the user decides to manually scrub through the animation, the timeline “at \_ days” statement will adjust in real time (**Fig. 35**).

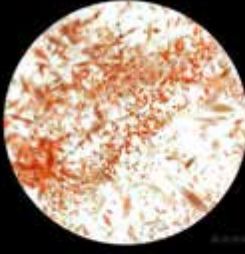
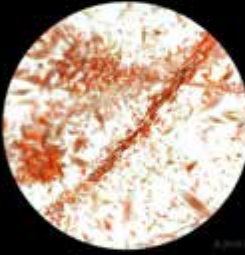

Oxygen level selected Time (days)	MP4 Visualization
<ul style="list-style-type: none"> <li>Normoxia (20% Oxygen)</li> </ul> <b>Angiogenesis at 0.0 days</b>	
<ul style="list-style-type: none"> <li>Hypoxia (2% Oxygen)</li> </ul> <b>Angiogenesis at 0.0 days</b>	
<ul style="list-style-type: none"> <li>Normoxia (20% Oxygen)</li> </ul> <b>Angiogenesis at 6.9 days</b>	
<ul style="list-style-type: none"> <li>Hypoxia (2% Oxygen)</li> </ul> <b>Angiogenesis at 7.9 days</b>	
<ul style="list-style-type: none"> <li>Normoxia (20% Oxygen)</li> </ul> <b>Angiogenesis at 14.0 days</b>	
<ul style="list-style-type: none"> <li>Hypoxia (2% Oxygen)</li> </ul> <b>Angiogenesis at 16.3 days</b>	

Figure 35: Table depicting the Time (days) and MP4 visualization based on the selected oxygen level.

### Angiogenesis Presentation Feedback

A rendered draft of the angiogenesis animation was presented to Dr. Warren Grayson and Juan Garcia for feedback. Dr. Grayson attested mainly to the scientific strength and similarity to how his laboratory aimed to classify the steps of angiogenesis. Dr. Warren Grayson's comments suggest that for future reiterations, the bone progenitor cells should be rendered a markedly different color from the vascular progenitor cells, as they were initially difficult to visually identify. In addition, bone progenitor cells would preferably be more numerous and pericytes would have longer cellular appendages that

would wrap more around the vasculature. To remedy this, a test render animatic coupled with some lit render stills would have allowed for feedback and edits before the final render.

Juan Garcia, the advisor for this thesis, made the observation that it is very difficult to determine how the two animations are dissimilar when presented apart from one another. It was suggested that they instead be shown side by side. The author agrees that this would be a viable suggestion moving forward.



### **Access to assets resulting from this thesis**

Access to the animation and interactive resulting from this thesis can be obtained by contacting the author at [ktang@jhmi.edu](mailto:ktang@jhmi.edu). The author may also be reached through the Department of Arts as Applied to Medicine via the website <http://www.medicalart.johnshopkins.edu/>.

## CONCLUSION

The progress of biomaterials in medicine is a formidable and fast-paced area of study. Concurrently with rapid innovations in biomaterial science, the public is well informed of and embracing of 3D printing technologies. However, there is a marked foreseeable lack of visual tools to communicate scientific findings and implications at the intersection of these two areas of research.

The visualizations and interactive presentation within this thesis aimed to connect the layman, medical, and scientific viewership to the great potential of 3D-printed bony scaffolds and vascular regeneration. In addition, the interactive presentation sought to provide the audience with a responsive method in which to observe the dynamic process of angiogenesis, one of the key components of biological regeneration. Although there is much more room for further development, the results of this project completed its objectives of providing storytelling visuals through which to communicate this novel area of complex scientific progress. For the angiogenesis interactive presentation, there is further progress to be made in terms of accuracy, complexity and immersiveness. However, the chosen presentation format addresses ease of accessibility and how to reach a broad target audience.

# APPENDIX

## Appendix A. List of Software

### SOFTWARE UTILIZED

<b>Program</b>	<b>Manufacturer</b>	<b>Manufacturer Headquarters</b>
Cinema 4D™	MAXON™	Friedrichsdorf, Germany
Photoshop CC 2015®	Adobe® Systems Inc.	San Jose, California
After Effects CC 2015®	Adobe® Systems Inc.	San Jose, California
Media Encoder CC 2015®	Adobe® Systems Inc.	San Jose, California
Audition CC 2015®	Adobe® Systems Inc.	San Jose, California
OsiriX, MD™	Pixmeo SARL®	Geneva, Switzerland
Zbrush®	Pixelogic®	Los Angeles, California
Meshlab™	ISTI-CNR Research Center	Pisa, Italy
Audacity® 2.1.2	The Audacity Team	Pittsburgh, Pennsylvania
Notepad®	Microsoft® Corp.	Redmond, Washington

### HARDWARE UTILIZED

<b>Hardware</b>	<b>Manufacturer</b>	<b>Manufacturer Headquarters</b>
27" desktop XPS® PC with 8GB RAM	Dell® Inc.	Round Rock, Texas
27" iMac® desktop with 8GB RAM	Apple® Inc.	Cupertino, California
Intuos 4® 6" x 8" graphics tablet	Wacom® Co.	Kazo, Saitama, Japan
Zoom H4n® digital recorder	Zoom® Corp.	Tokyo, Japan

## Appendix B. Part I Final Animation in Storyboard Format

**Project:** *Regenerating Vascularized Craniofacial Bone with 3D-Printed Porous Scaffolds and Stromal-vascular Fraction Cells.*  
**Client:** Dr. Warren Grayson


**Sequence:** **I. Anatomically shaped graft is essential for functional CMF regeneration.**

**001**

Regenerating Vascularized Craniofacial Bone with 3D-Printed Porous Scaffolds and Stromal-vascular Fraction Cells

Start: \_\_\_\_\_ Stop: \_\_\_\_\_  
 Video: \_\_\_\_\_

**002**




Start: \_\_\_\_\_ Stop: \_\_\_\_\_  
 Video: \_\_\_\_\_

**003**

SURGICAL RECONSTRUCTION USING BONE GRAFTS

Autograft  
 Allograft  
 Xenograft



Start: \_\_\_\_\_ Stop: \_\_\_\_\_  
 Video: \_\_\_\_\_

**004**


Regenerating Vascularized Craniofacial Bone with 3D-Printed Porous Scaffolds and Stromal-vascular Fraction Cells.

Start: \_\_\_\_\_ Stop: \_\_\_\_\_  
 Video: \_\_\_\_\_

**005**

Autograft

The transfer of bone from one site to another within a single patient



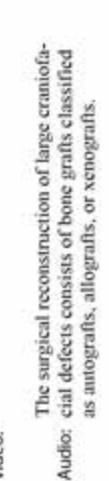
Start: \_\_\_\_\_ Stop: \_\_\_\_\_  
 Video: \_\_\_\_\_

**006**

Autograft

CONSTRAINTS:

- Limited bone for transfer
- Complex craniofacial structure




Start: \_\_\_\_\_ Stop: \_\_\_\_\_  
 Video: \_\_\_\_\_

**004**

Autograft

The transfer of bone from one site to another within a single patient




Start: \_\_\_\_\_ Stop: \_\_\_\_\_  
 Video: \_\_\_\_\_

**005**

Autograft

The transfer of bone from one site to another within a single patient




Start: \_\_\_\_\_ Stop: \_\_\_\_\_  
 Video: \_\_\_\_\_

**006**

Autograft

CONSTRAINTS:

- Limited bone for transfer
- Complex craniofacial structure



Start: \_\_\_\_\_ Stop: \_\_\_\_\_  
 Video: \_\_\_\_\_

**004**

The most common technique is an autograft, the transfer of bone from one site to another within a single patient....

Start: \_\_\_\_\_ Stop: \_\_\_\_\_  
 Video: \_\_\_\_\_

**005**

Audio: ...usually with a donor site from the iliac crest, ribs, or fibula.

Start: \_\_\_\_\_ Stop: \_\_\_\_\_  
 Video: \_\_\_\_\_

**006**

Audio: Autografts have many constraints, including a limited amount of bone that can be transferred and the task of aesthetically matching a complex facial structure at the site of defect.

Start: \_\_\_\_\_ Stop: \_\_\_\_\_  
 Video: \_\_\_\_\_

## Appendix B. Part I Final Animation in Storyboard Format (cont.)

Project: *Regenerating Vascularized Craniofacial Bone with 3D-Printed Porous Scaffolds and Stromal-vascular Fraction Cells*  
 Client: Dr. Warren Grayson

Sequence: **I. Anatomically shaped graft is essential for functional CMF regeneration.**



Start: \_\_\_\_\_ Stop: \_\_\_\_\_  
 Video: \_\_\_\_\_

The newest advances in 3D-printing biomaterials force a vastly improved surgical procedure that would allow the surgeon to graft a 3D-printed scaffold perfectly shaped to fit the patient.



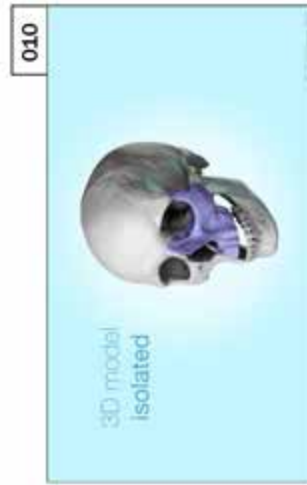
Start: \_\_\_\_\_ Stop: \_\_\_\_\_  
 Video: \_\_\_\_\_

Audio:



Start: \_\_\_\_\_ Stop: \_\_\_\_\_  
 Video: *Radiological imaging ->*

Audio: The scaffolds themselves are generated from the patient's CT scans ...



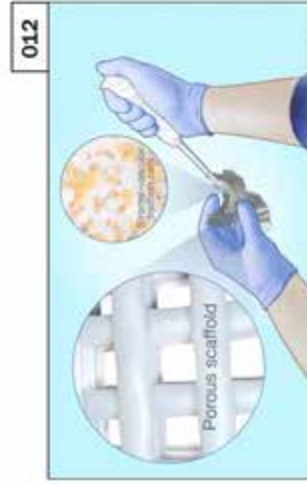
Start: \_\_\_\_\_ Stop: \_\_\_\_\_  
 Video: *3D Models -> 3D Printed*

from which the 3D models are then isolated.



Start: \_\_\_\_\_ Stop: \_\_\_\_\_  
 Video: *3D Models -> 3D Printed*

It is then printed using a 3D printer and a mixture of bone matrix and polycaprolactone (PCL), with embedded "microtanks" containing oxygen.



Start: \_\_\_\_\_ Stop: \_\_\_\_\_  
 Video: \_\_\_\_\_

From here, the scaffold is seeded with adipose-derived stem cells, before being implanted inside the patient.

**Appendix B. Part I Final Animation in Storyboard Format (cont.)**

**Project:** *Regenerating Vascularized Craniofacial Bone with 3D-Printed Porous Scaffolds and Stromal-vascular Fraction Cells.*  
**Client:** Dr. Warren Grayson

**Sequence:** **I. Anatomically shaped graft is essential for functional CMF regeneration.**



Start: \_\_\_\_\_ Stop: \_\_\_\_\_  
 Video: \_\_\_\_\_

Start: \_\_\_\_\_ Stop: \_\_\_\_\_  
 Video: \_\_\_\_\_

Together, this procedure provides a stream-lined surgical approach to reconstructing craniofacial defects.

## Appendix C. Angiogenesis Interactive Presentation: HTML and Javascript code

```
<html>
<head>
</head>

<body style="background-color:black;">

<br>

<div style="text-align:center; color:#f2664a; font-
weight:bold; font-size:48px;">Angiogenesis over Time (Days)
</div>

<div id="stage" style="text-align:center">
  <video src="http://www.kaioutang.com/img/angio_micro.mp4"
id="video1" width="800" muted="muted" controls></video>
</div>

<div style="text-align:center; color:#b0b0b0; font-
size:18px;"><i>Move the video slider left and right to see how
<br>oxygen levels affect vessel growth time (days):</i></div>

<div id="time" style="text-align:center; color:#f2664a; font-
weight:bold; font-size:32px;">Angiogenesis at 0.0 days</div>

<form action="#" method="post" class="Form" id="oxySelect">
<div style="text-align:center; color:white; font-
size:24px;"><b>Select oxygen parameters:</b></div>
<div style="text-align:center; color:white; font-weight:bold;
font-size:20px;">
  <label><input type="radio" name="group1" value="0.829"
checked /> Normoxia (20% Oxygen)</label><br>
  <label><input type="radio" name="group1" value="0.966"
/> Hypoxia (2% Oxygen)</label><br>
</div>
</form>

<br><br><br><br>

<div style="color:white; font-size:16px;">
<i>Source: <br>
Hutton DL, Logsdon EA, Moore EM, Gabhann FM, Gimble JM,
Grayson WL. <b>Vascular morphogenesis of adipose-derived stem
cells is mediated by heterotypic cell-cell interactions.
</b>Tissue Engineering Part A. 2012; 18:1729-1740.</i></div>
```

## Appendix C. Angiogenesis Interactive Presentation: HTML and Javascript code (cont.)

```
<script type="text/javascript">
(function(){
  var v = document.getElementsByTagName('video')[0]
  var t = document.getElementById('time');
  var x = 0.829;

  // Oxygen level onclick
  var group1 = document.forms['oxySelect'].
elements['group1'];

  for (var i=0, len=group1.length; i<len; i++) {
    group1[i].onclick = function() {
      x=this.value;
      t.innerHTML = ' Angiogenesis at ' + parseFloat(v.
currentTime*x).toFixed(1) + ' days ' ;
    };
  }

  for (var i=0, len=document.forms.length; i<len; i++) {
    document.forms[i].onsubmit = function() { return
false; };
  }

  v.addEventListener('timeupdate',function(event){
    t.innerHTML = ' Angiogenesis at ' + parseFloat(v.
currentTime*x).toFixed(1) + ' days '
    },false);
})();
</script>
</div>

</body>
</html>
```



## Appendix D. Part I Animation Storyboards

Project: *Regenerating Vascularized Craniofacial Bone with 3D-Printed Porous Scaffolds and Adipose-derived Stem Cells.*  
 Client: Dr. Warren Grayson

Sequence: **Anatomically shaped graft is essential for functional CMF regeneration.**

**1**

**Regenerating Vascularized Craniofacial Bone with 3D-Printed Porous Scaffolds and Adipose-derived Stem Cells.**

Start: \_\_\_\_\_ Stop: \_\_\_\_\_  
 Video: \_\_\_\_\_


**2**

**Autografts - Allografts - Xenografts**

Start: \_\_\_\_\_ Stop: \_\_\_\_\_  
 Video: *Image*

**3**

**Autografts**  
(define)

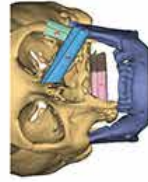


Start: \_\_\_\_\_ Stop: \_\_\_\_\_  
 Video: *Image*

The most common technique is an autograft, the transfer of bone from one site to another within a single patient, usually with a donor site from the iliac crest, ribs, or fibula.

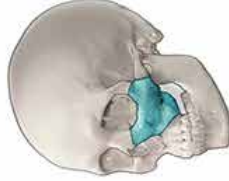
The surgical reconstruction of large craniofacial defects consists of bone grafts classified as autografts, allografts, or xenografts.

**4**



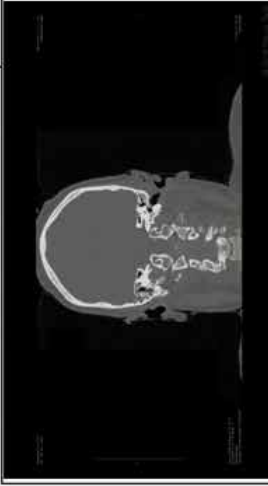
Start: \_\_\_\_\_ Stop: \_\_\_\_\_  
 Video: *Image*

**5**



Start: \_\_\_\_\_ Stop: \_\_\_\_\_  
 Video: \_\_\_\_\_

**6**



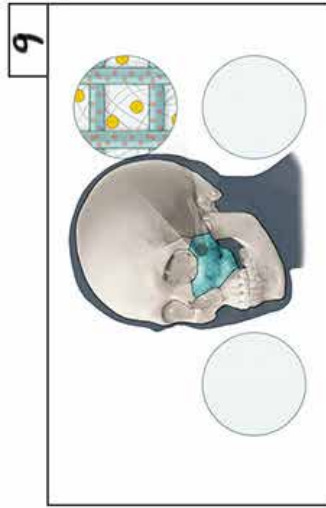
Start: \_\_\_\_\_ Stop: \_\_\_\_\_  
 Video: \_\_\_\_\_

Autografts have many constraints, including a limited amount of bone that can be transferred and the task of aesthetically matching a complex facial structure at the site of defect.

The newest advances in 3D-printing biomaterials foresee a vastly improved surgical procedure that would allow the surgeon to graft a 3D-printed scaffold perfectly shaped to fit the patient.

Audio: Radiological imaging ->  
 The scaffolds themselves are generated from the patient's CT scans ...

Appendix D. Part I Animation Storyboards (cont.)



Start: \_\_\_\_\_ Stop: \_\_\_\_\_  
 Video: *Image*

From here, the scaffold is seeded with adipose-derived stem cells, before being implanted inside the patient. Together, this procedure provides a streamlined surgical approach to reconstructing craniofacial defects.



Start: \_\_\_\_\_ Stop: \_\_\_\_\_  
 Video: *3D Models->3D Printed*

It is then printed using a 3D printer and a mixture of bone matrix and polycaprolactone (PCL), with embedded "microtanks" containing oxygen.



Start: \_\_\_\_\_ Stop: \_\_\_\_\_  
 Video: *3D Models->3D Printed*

from which the 3D models are then isolated.

## Appendix E. Part II Animation Storyboards

Project: *Regenerating Vascularized Craniofacial Bone with 3D-Printed Porous Scaffolds and Adipose-derived Stem Cells.*  
 Client: Dr. Warren Grayson  
 Sequence: **The 3D-printed scaffold before implantation**

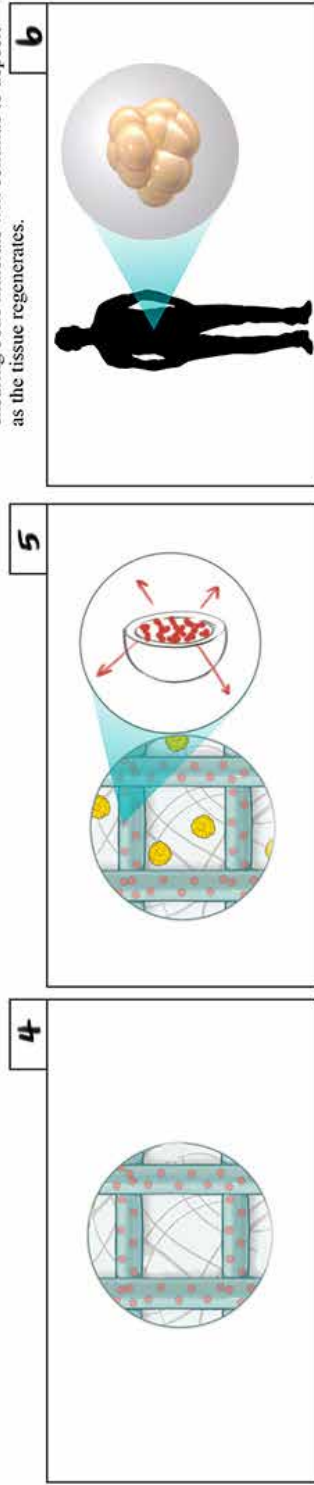


Start: \_\_\_\_\_ Stop: \_\_\_\_\_  
 Video: *Image* Video: \_\_\_\_\_ Stop: \_\_\_\_\_

Once a scaffold has been printed to fit the patient's face, how does this regenerate into organic bone tissue?

The 3D-printed scaffold is made up of two main components: (2) Oxygen microtanks, and (3) Bone matrix cues, to which (1) Adipose-derived stem cells are added.

Bone matrix cues have been mixed into the scaffold when printed. Here, the presence of calcium phosphate and collagen are essential to ensuring bone minerals will continue to deposit as the tissue regenerates.




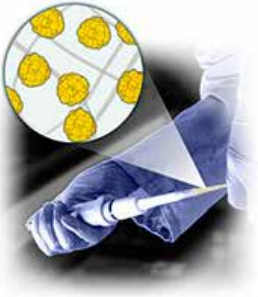
Start: \_\_\_\_\_ Stop: \_\_\_\_\_  
 Video: *Image* Video: \_\_\_\_\_ Stop: \_\_\_\_\_

Oxygen concentration is a critical factor in cell survival and vessel formation, thus, an oxygen supply within the scaffold is crucial.

The scaffold is melt-mixed and 3D-printed with oxygen microtanks, microscopic hollow balloons. After printing, the scaffolds are hyperbarically loaded with oxygen for diffusion after implantation.

(1) Adipose-derived stem cells, (2) Adipose-derived stem cells, from fat tissue, are acquired through liposuction, where fat is taken from the abdomen, thighs, or buttocks.

**Appendix E. Part II Animation Storyboards (cont.)**

<p><b>7</b></p>  <ol style="list-style-type: none"> <li>1. Heterogeneity</li> <li>2. Vascular assembly</li> <li>3. Ease of acquisition</li> </ol>	<p><b>8</b></p> 
--	---

**Start:** \_\_\_\_\_ **Stop:** \_\_\_\_\_

**Video:** Adipose-derived stem cells have been identified as a suitable cell type for bone tissue regeneration, due to the (1) ease of acquisition of large quantities of stem cells, (2) heterogeneity (that is, the presence of multiple cell types including vascular phenotypes and osteogenic progenitors), and (3) the ability of these multiple cells types to self-assemble into vascular networks, which will form the templates for new mineral deposition

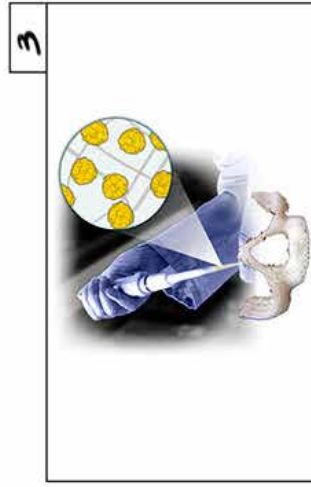
**Start:** \_\_\_\_\_ **Stop:** \_\_\_\_\_

**Video:** Just prior to surgical implantation, the adipose-derived stem cells, in a fibrin gel, are pipetted onto the 3D-printed scaffold.

# Appendix F. Part III Animation Storyboards

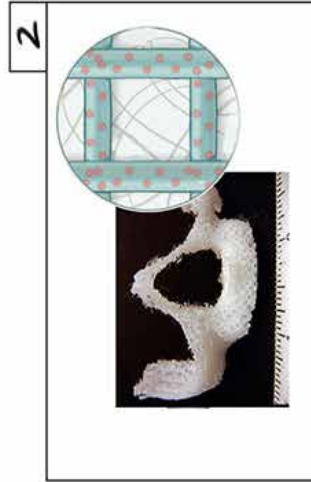
Project: *Regenerating Vascularized Craniofacial Bone with 3D-Printed Porous Scaffolds and Adipose-derived Stem Cells.*  
 Client: Dr. Warren Grayson

Sequence: **The regeneration process from 3D-printed scaffold to organic bone tissue**



Start: \_\_\_\_\_ Stop: \_\_\_\_\_  
 Video: \_\_\_\_\_

2. Extraction of adipose-derived stem cells that are placed into the pre-fabricated scaffold and immediately transplanted to the bone defect site.



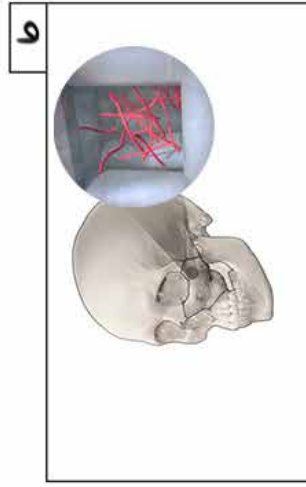
Start: \_\_\_\_\_ Stop: \_\_\_\_\_  
 Video: \_\_\_\_\_

Bone regeneration occurs through six stages:  
 Audio: 1. The use of a pre-fabricated, biodegradable, porous scaffold that provides structure to guide the shape of the regenerating bone tissue.



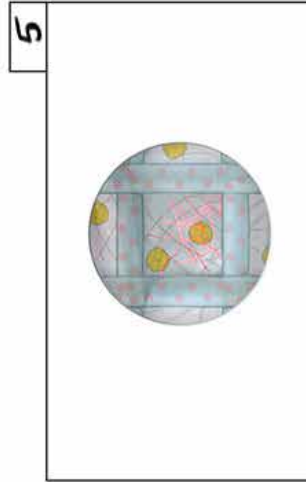
Start: \_\_\_\_\_ Stop: \_\_\_\_\_  
 Video: \_\_\_\_\_

Once a scaffold has been printed to fit the patient's face, how does this regenerate into organic bone tissue?



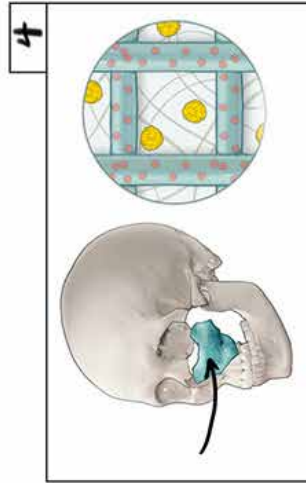
Start: \_\_\_\_\_ Stop: \_\_\_\_\_  
 Video: *Image*

Audio: 6. Degradation of the scaffold leaving only biological bone replacement that responds to physiological signals.



Start: \_\_\_\_\_ Stop: \_\_\_\_\_  
 Video: \_\_\_\_\_

Audio: 4. Formation of new blood vessels from transplanted stem cells. These will connect with existing blood vessels from neighboring tissues to provide a continuous blood supply.  
 5. Differentiation of fat stem cells into bone forming cells, and deposition of new mineral to fill the pore spaces.



Start: \_\_\_\_\_ Stop: \_\_\_\_\_  
 Video: \_\_\_\_\_

Audio: 3. Controlled delivery of oxygen from the scaffold to maintain stem cell survival using oxygen microtanks.

# Appendix G. Part IV Animation Storyboards

Project: *Regenerating Vascularized Craniofacial Bone with 3D-Printed Porous Scaffolds and Adipose-derived Stem Cells.*  
 Client: Dr. Warren Grayson  
 Sequence: **1-Day Clinical procedure**

**1**



Start: \_\_\_\_\_ Stop: \_\_\_\_\_  
 Video: *1-Day Clinical procedure*

Audio: In summary, first...

**2**



Start: \_\_\_\_\_ Stop: \_\_\_\_\_  
 Video: *Clinical image*

Audio: 1. CT scans are taken of the patient

**3**



Start: \_\_\_\_\_ Stop: \_\_\_\_\_  
 Video: *Anatomically-shaped model*

Audio: 2. From which an anatomically-shaped scaffold is created.

**4**



Start: \_\_\_\_\_ Stop: \_\_\_\_\_  
 Video: *3D Print scaffold*

Audio: 3. The model is then 3D-printed into a scaffold, which is then packaged and sent to the operating room.

**5**



Start: \_\_\_\_\_ Stop: \_\_\_\_\_  
 Video: *Seed ADP cells*

Audio: 4. The surgeon adds the lipoaspirated adipose-derived stem cells to the scaffold in a sterile environment.

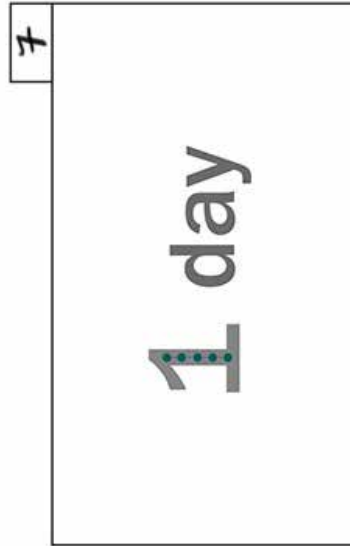
**6**



Start: \_\_\_\_\_ Stop: \_\_\_\_\_  
 Video: *Surgical implant*

Audio: 5. and surgically implants it into the patient.

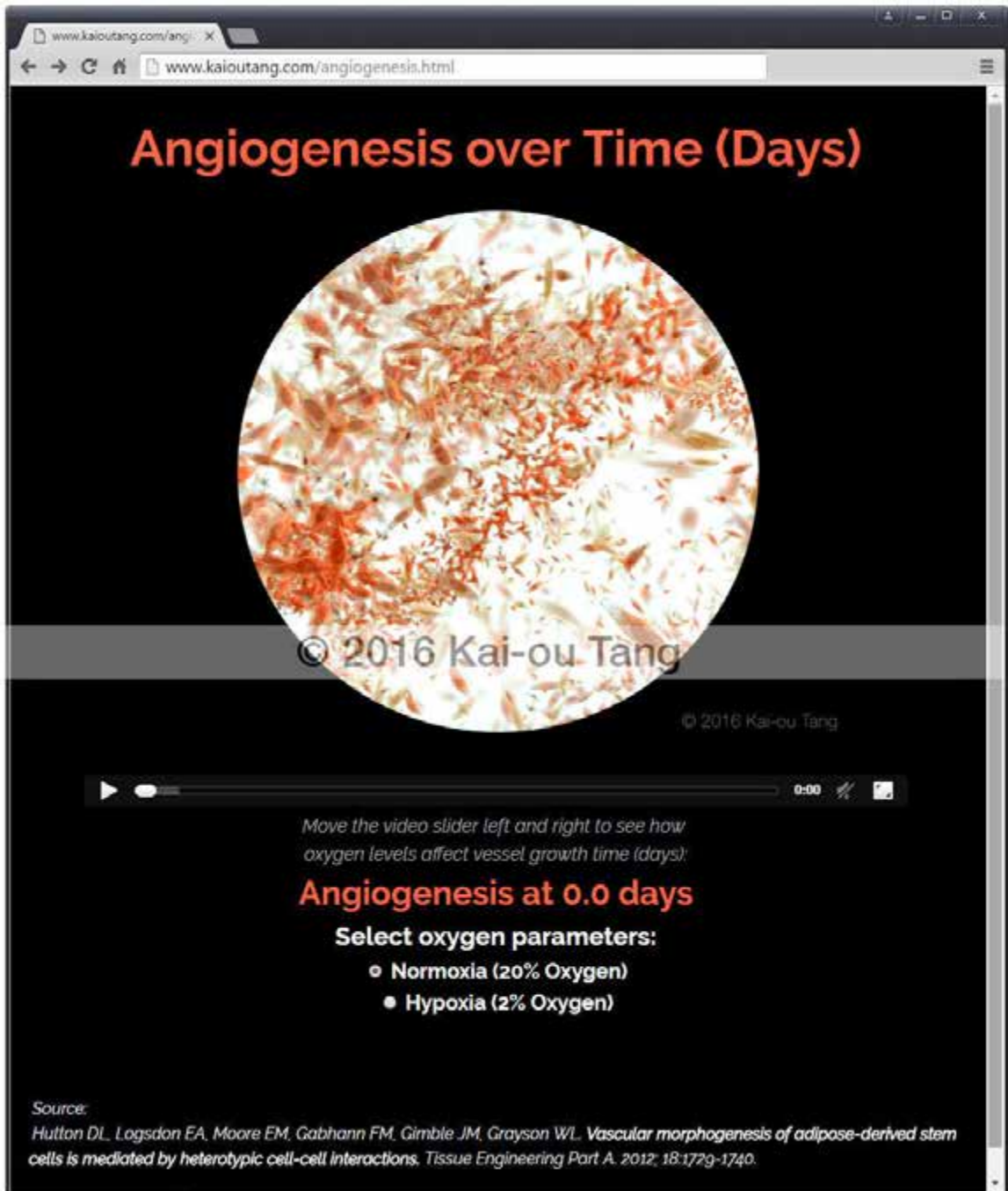
**Appendix G. Part IV Animation Storyboards (cont.)**



Start: \_\_\_\_\_ Stop: \_\_\_\_\_  
Video: *1-Day Clinical procedure*

Audio: The entire clinical process from start to finish spans only one day!

## Appendix H. Part V Angiogenesis Interactive Presentation



www.kaioutang.com/angiogenesis.html

# Angiogenesis over Time (Days)

© 2016 Kai-ou Tang

© 2016 Kai-ou Tang

0:00

Move the video slider left and right to see how oxygen levels affect vessel growth time (days):

## Angiogenesis at 0.0 days

Select oxygen parameters:

- Normoxia (20% Oxygen)
- Hypoxia (2% Oxygen)

Source:  
Hutton DL, Logsdon EA, Moore EM, Gabhann FM, Gimble JM, Grayson WL. Vascular morphogenesis of adipose-derived stem cells is mediated by heterotypic cell-cell interactions. *Tissue Engineering Part A*. 2012; 18:1729-1740.



## Appendix I. Part V Angiogenesis Interactive Presentation Time Lapse



## Appendix I. Part V Angiogenesis Interactive Presentation Time Lapse (cont.)



## Appendix J. Part I-IV Narration Script

“Regenerating Vascularized Craniofacial Bone with 3D-Printed Porous Scaffolds and Stromal Vascular Fraction Cells.”

(PART I) An anatomically-shaped graft is essential for functional craniofacial bone regeneration. The surgical reconstruction of large craniofacial defects consists of bone grafts classified as autografts, allografts, or xenografts.

The most common technique is an autograft, the transfer of bone from one site to another within a single patient, usually from the iliac crest, ribs, or fibula. Autografts have many constraints, including a limited amount of bone that can be transferred and the task of aesthetically matching a complex facial structure at the site of defect.

The newest advances in 3D-printing biomaterials foresee a vastly improved surgical procedure that would allow the surgeon to graft a 3D-printed scaffold custom-shaped to fit the patient.

The scaffolds are generated and sculpted using the patient’s CT scans, from which the 3D models are then isolated.

It is then 3D-printed using a mixture of bone matrix and polycaprolactone (or PCL), with embedded “microtanks” containing oxygen.

From here, the scaffold is seeded with stromal vascular fraction cells which contain adipose-derived stem cells, before being implanted inside the patient. Together, this procedure provides a streamlined surgical approach to reconstructing craniofacial defects.

## Appendix J. Part I-IV Narration Script (cont.)

(PART II) The 3D-printed scaffold before implantation

The 3D-printed scaffold is made up of two main components: Oxygen microtanks, and Bone matrix cues, to which Adipose-derived stem cells are added.

(1) Adipose-derived stem cells ,  
Adipose-derived stem cells, from fat tissue, are acquired through lipoaspiration, where fat is taken from the abdomen, thighs, or buttocks. Adipose-derived stem cells have been identified as a suitable cell type for bone tissue regeneration, due to the (1) ease of acquisition of large quantities of stem cells. (2) heterogeneity (that is, the presence of multiple cell types including vascular phenotypes and osteogenic progenitors), and (3) the ability of these multiple cells types to self-assemble into vascular networks, which will form the templates for new mineral deposition.

(2) Oxygen microtanks

Oxygen concentration is a critical factor in cell survival and vessel formation, thus, an oxygen supply within the scaffold is crucial.

The scaffold is melt-mixed and 3D-printed with oxygen microtanks, microscopic hollow balloons. After printing, the scaffolds are hyperbarically loaded with oxygen for diffusion after implantation.

(3) Bone matrix cues

Bone matrix cues have been mixed into the polycaprolactone and are incorporated into the scaffold when printed.

Here, the presence of calcium phosphate and collagen are essential to ensuring bone minerals will continue to deposit as the tissue regenerates.

Just prior to surgical implantation, the adipose-derived stem cells, in a fibrin gel, are pipetted onto the 3D-printed scaffold.

## Appendix J. Part I-IV Narration Script (cont.)

(PART III) The Regeneration Process from 3D-printed Scaffold to Organic Bone Tissue.

Once a scaffold has been printed to fit the patient's face, how does this regenerate into organic bone tissue?

Bone regeneration occurs through six stages:

1. The use of a pre-fabricated, biodegradable, porous scaffold that provides structure to guide the shape of the regenerating bone tissue.
2. Extraction of adipose-derived stem cells that are placed into the pre-fabricated scaffold and immediately transplanted to the bone defect site.
3. Controlled delivery of oxygen from the scaffold to maintain stem cell survival using oxygen microtanks.
4. Formation of new blood vessels from transplanted stem cells. These will connect with existing blood vessels from neighboring tissues to provide a continuous blood supply.
5. Differentiation of fat stem cells into bone forming cells, and deposition of new mineral to fill the pore spaces.
6. Degradation of the scaffold leaving only biological bone replacement that responds to physiological signals.

## Appendix J. Part I-IV Narration Script (cont.)

(PART IV) The workflow from CT scan to operation

In summary, first...

1. CT scans are taken of the patient.
2. From which an anatomically-shaped scaffold model is created.
3. The model is then 3D-printed into a scaffold, which is then packaged and sent to the operating room.
4. The surgeon adds the lipoaspirated adipose-derived stem cells to the scaffold in a sterile environment,
5. and surgically implants it into the patient.

The entire clinical process from start to finish spans only one day.

## REFERENCES

- Ariens RAS. "Counting 1 fibrin molecule at a time." *Blood*. 2013; 121 (8): 1251-1252.
- Cook CA, Hahn KC, Morrissette-McAlmon JFB, Grayson WL. "Oxygen delivery from hyperbarically loaded microtanks extends cell viability in anoxic environments." *Biomaterials*. 2015; 52:376-384.
- Correia C, Grayson WL, Park M, Hutton D, Zhou B, Guo XE, Niklason L, Sousa RA, Reis RL, Vunjak-Novakovic G. "In Vitro Model of Vascularized Bone: Synergizing Vascular Development and Osteogenesis." *PLoS ONE*. 2011; 6(12):1-9.
- DICOM Sample Image Sets. Pixmeo SARL®, 2014. Web. Nov. 2015. <<http://www.osirixviewer.com/datasets/>>.
- Donati D, Zolezzi C, Tomba P, Viganò A. "Bone grafting: historical and conceptual review, starting with an old manuscript by Vittorio Putti." *Acta Orthopaedica*. 2007; 78(1):19-25.
- Elsalanty ME, Genecov DG. "Bone grafts in craniofacial surgery." *Craniofacial Trauma & Reconstruction*. 2009; 2(3):125-134.
- Ge J, Guo L, Wang S, Zhang Y, Cai T, Zhao RCH, Wu Y. "The Size of Mesenchymal Stem Cells is a Significant Cause of Vascular Obstructions and Stroke." *Stem Cell Reviews and Reports*. 2007; 10 (2):295-303.
- Hung BP, Salter EK, Temple J, Mundinger GS, Brown EN, Brazio P, Rodriguez ED, Grayson WL. "Engineering Bone Grafts with Enhanced Bone Marrow and Native Scaffolds." *Cells Tissues Organs*. 2013;198:87-98.
- Gomes KU, Rapoport A, Carlini JL, Lehn CN, Denardin OV. "Social integration and inclusion after pre-maxilla surgical repositioning in patients with bilateral cleft palate and lip." *Brazilian Journal of Otorhinolaryngology*. 2009;75(4):537-43.
- Huri PY, Cook CA, Hutton DL, Goh BC, Gimble JM, DiGirolamo DJ, Grayson WL. "Biophysical cues enhance myogenesis of human adipose derived stem/stromal cells." *Biochemical and Biophysical Research Communications*. 2013; 438(1): 180-185.
- Hutton DL, Logsdon EA, Moore EM, Gabhann FM, Gimble JM, Grayson WL. "Vascular morphogenesis of adipose-derived stem cells is mediated by heterotypic cell-cell interactions." *Tissue Engineering*. 2012; 18:1729-1740.
- Lawson, Bruce, and Remy Sharp. "HTML5 Audio and Video: What You Must Know." EnvatoTuts. October 25, 2010. Accessed March 10, 2016. <<http://code.tutsplus.com/tutorials/html5-audio-and-video-what-you-must-know--net-15545/>>.

- O’Keefe R. “Fibrinolysis as a Target to Enhance Fracture Healing.” *The New England Journal of Medicine*. 2015; 373(18):1776-1778.
- “Radio Button Onclick vs. Onchange Event.” Dynamic Web Coding. 2001. Accessed March 10, 2016. <<http://www.dyn-web.com/tutorials/forms/radio/onclick-onchange.php/>>.
- Singh AK, Mohapatra DP, Kumar V. “Spectrum of primary bone grafting in cranio maxillofacial trauma at a tertiary care centre in India.” *Indian Journal of Plastic Surgery*. 2011; 44(1):29-35.
- Tzeng SY, Hung BP, Grayson WL, Green JJ. “Cystamine-terminated poly(beta-amino ester)s for siRNA delivery to human mesenchymal stem cells and enhancement of osteogenic differentiation.” *Biomaterials*. 2012; 33(32): 8142–8151.
- Temple JP, Hutton DL, Hung BP, Huri PY, Cook CA, Kondragunta R, Jia X, Grayson WL. “Engineering anatomically shaped vascularized bone grafts with hASCs and 3D-printed PCL scaffolds.” *Journal of Biomedical Materials Research*. 2014;102A:4317–4325.
- Velaga, Mahesh. “Parse Float with Two Decimal Places.” Stack Overflow. December 14, 2010. Accessed March 10, 2016. <<http://stackoverflow.com/questions/4435170/parse-float-with-two-decimal-places/>>.
- Vunjak-Novakovic, Gordana, and Kursad Turksen. *Biomimetics and Stem Cells: Methods and Protocols*. New York: Humana Press, 2014.
- Zhang S, Liu X, Barreto-Ortiz SF, Yu T, Ginn B, DeSantis N, Hutton DL, Grayson WL, Cui F, Korgei BA, Gerecht S, Mao H. “Creating Polymer Hydrogel Microfibres with Internal Alignment via Electrical and Mechanical Stretching.” *Biomaterials*. 2014; 35(10): 3243–3251.



## VITA

Kai-ou Tang was born in 1987 in Montreal, Canada, to parents both working in the life sciences. Their careers led them to frequent relocations, and Kai-ou spent her elementary school years in the United Kingdom, California, and Colorado, before moving to North Carolina. It was there that she enrolled at the University of North Carolina at Chapel Hill, studying for a Bachelor of Arts in Biology.

In 2011, Kai-ou relocated to Boston, MA, where she was a summer intern at the Pediatrics Division of Harvard Medical School/Mass General Hospital, researching the helminth parasite and its immunological response. After the internship ended, she entered the field of Histotechnology, working at Boston Medical and MetaMark Genetics as an Immunohistochemistry Histotechnician, attaining her Histotechnologist certification in 2014.

That same year, she was matriculated into the Johns Hopkins School of Medicine graduate program in Medical and Biological Illustration in Baltimore, MD. She is grateful for the steady support of faculty and peers, and the tight-knit relationships formed over the short two years.

Following the attainment of her Master of Arts degree in May 2016, Kai-ou hopes to pursue her interest in 3D modeling, animation, medical device design, and scientific illustration.